

Investigating Plasmons with Total Internal Reflection Microscopy

A Thesis Presented to the
Faculty of the Department of Chemistry, Bates College
In partial fulfillment of the requirements for the
Degree of Bachelor of Science

Blaise Jonathan Thompson
April 14, 2011

Acknowledgments

This thesis document, and the lab work that it represents, would have been much less of a success without the help of my advisor Matthew Côté and my lab associates Elliott Morgan and Jacob Simon. The process of producing this work would have been much less joyful and productive without the constant presence and assistance of my roommate Claire Parker.

Contents

1	Introduction	7
1.1	The very small	7
1.2	The plasmon polariton	8
1.2.1	Plasmon polaritons and fluorescence	9
1.3	Total internal reflection	10
1.4	Atomic force microscopy	11
1.5	Our instrument	11
2	Background	15
2.1	Plasmons	15
2.1.1	Introduction; the surface plasmon polariton (SPP) . .	15
2.1.2	Localized surface plasmon resonance (LSPR)	21
2.1.3	Plasmon-polaritons as scatterers; the spectrum of a plasmon	21
2.1.4	Crystal momentum & plasmon-polaritons	21
2.2	Optics	22
2.2.1	Index of refraction, bending light	22
2.2.2	Lenses and magnification	23
2.2.3	Numerical aperture, resolving power & the diffraction limit	24
2.2.4	Köhler illumination	25
2.2.5	Total internal reflection (TIR)	25
2.2.6	Optical dispersion, the grism	28
2.3	Fluorescence	30
2.3.1	Selection rules & energy	30
2.3.2	Metal enhanced fluorescence & the Purcell effect . .	30
3	Experimental	33
3.1	Total internal reflection microscope	33

3.1.1	Input optics & sources	33
3.1.2	Objective, input mirrors, & sample mount	35
3.1.3	Output optics, imaging & spectroscopy	36
3.1.4	Improving image quality and the signal to noise ratio	39
3.1.5	Integration with AFM	41
3.2	Fluorescence investigations	41
3.2.1	Fluorescent nanospheres	41
3.2.2	Dye coated surface	42
3.3	Plasmonic investigations	42
3.3.1	UV-Vis absorption spectra of gold nanorods	42
3.4	Imaging of gold nanorods	43
3.5	Nanosphere lithography	43
4	Results & Discussion	45
4.1	Instrumental successes	45
4.2	Plasmonic investigations	47
4.2.1	Imaging of gold nanorods	47
4.2.2	UV-Vis absorption spectra of gold nanorods	47
4.3	Fluorescence	48
4.3.1	Viewing fluorescence with TIR	48
4.3.2	Cresyl-blue coated surface	49
4.3.3	Nanosphere lithography	51
4.4	Conclusion, looking forward	51
A	The instrument	57

Chapter 1

Introduction

1.1 The very small

Our knowledge of the nanoworld (roughly the scale of 10^{-9} meters, *one billionth* of a meter) has grown greatly in the last twenty years. The tools that we have for manipulating and observing nano-objects have become more and more sophisticated, and applications of nano-objects and nano-tools have already become ubiquitous in biology, medicine, chemistry, and physics. Still, we have only scratched the surface — the nanoworld still holds much interest and promise to scientists.

Electro-magnetic fields have become an everyday tool for humans, so much so that some have questioned the safety of being constantly bathed in electro-magnetic waves from power lines, radio towers and fluorescent light bulbs. Electro-magnetic radiation (light) has been used for centuries to create images of objects and to excite and investigate physical systems. With the invention of the laser in 1960, a new field called photonics was born and new exciting uses for light came to the table. Today, light is used as an information carrier in a widespread network of fiber-optic telecommunication cables.

Scientists and engineers would like to take the information carrying, image generating, energy probing power of light and apply it to the nanoscale. This is no trivial task; there are fundamental difficulties involved in shrinking electro-magnetic waves with wavelengths on the scale of hundreds of nanometers into volumes in the tens of cubic nanometers. By achieving these small volumes, it would be possible to open up even more exiting uses for light.

One successful technique for trapping electro-magnetic waves in nanome-

ter volumes and directing their flow has been to trap the waves at the surface of metals using plasmons, nanoscale electron excitations.

1.2 The plasmon polariton

Plasmons are quanta of plasma oscillation. They take the form of propagating waves of electron density in conducting solids. Plasmonic systems are inherently dynamic—the waves of electron density constantly move and change in phase and magnitude. The shape, magnitude and direction of propagation of plasmons can be tuned by altering the environment of the plasmon(most easily done by altering the *shape* or *composition* of the SPP supporting object.) It is partially because of this tuneability that plasmons are so promising as tools.

Plasmons that are confined to the surface of a conductor — surface plasmons — are the most studied variety of plasmons. Surface plasmons are always accompanied by an associated electromagnetic field called the polariton. These surface plasmon polaritons (SPPs) are waves of oscillating electrons and photons that propagate along interfaces between metals and non-conducting (dielectric) materials. The plasmon is made up of regions of high and low electron density, while the polariton is the associated electromagnetic field caused by the charge distribution. The polariton extends from the surface into both the dielectric medium and the metal [2], as shown on the right-hand side of figure 2.1.

The existence of SPPs was predicted by R. H. Ritche in his 1957 paper Plasma Losses by Fast Electrons in Thin Films [18]. Since then, many groups have hopped on the surface plasmon polariton bandwagon, and many SPP-based devices have been proposed. Waveguides, photonic circuits, molecular rulers, and chemical sensors are just a few of the SPP based devices that could revolutionize both science and industry if actualized [12].

Recently, groups have reported detailed theoretical descriptions of surface plasmon polaritons in simplified situations, like SPPs on an infinite plane of metal ([17], [26]). These are great steps forward, but theory alone is not sufficient for scientific and technological process. Experimental measurements of surface plasmon polaritons in various environments is necessary. More explicitly, one crucial next step is to map the electromagnetic field of single plasmon polaritons in known physical situations. Detailed measurements are necessary to validate and refined current theory, and the tools and experiments devised to make those measurements will push forward our ability to create, sustain, and manipulate plasmon polaritons in

novel situations.

There have already been some initial forays into mapping the electro-magnetic field of plasmon polaritons. Attempts and successes at mapping the electro-magnetic field of SPPs in metal films ([24], [14]) nanostructures ([3]) and even simple optical circuits [4] have already led to applications like plasmon-enhanced spectroscopy ([16]), light emission, [24] and light emitting diodes ([16], [23]). These initial successes point towards a rich region of research in plasmon polariton associated electro-magnetic field mapping.

The work represented in this thesis builds on the work of Weeber *et. al* [25] by constructing an instrument that utilizes an atomic force microscope and an optical microscope using total internal reflection to map the electro-magnetic field of surface plasmon polaritons. Both are proven techniques for observing plasmon polaritons, and when brought together they offer some unique advantages that allow cutting edge measurements.

1.2.1 Plasmon polaritons and fluorescence

One of the multitude of investigations into SPPs as tools is the attempt to understand the interaction between SPPs and fluorescence. Surface plasmon polaritons can interact with fluorescent molecules in two ways: 1) the strong electro-magnetic field can excite electrons to higher states and 2) the plasmon and associated phonons in the metal can quench the radiative release of energy in the form of a photon via a non-radiative energy transfer(see 2.3.2 for more). These two conflicting interactions have led to seemingly contradictory observations. Some papers report more fluorescence as molecules interact with SPPs ([20], [13]), some report less ([6], [21]), and still others report varied results ([1]). Investigating the data reveals a trend: the relative degree of excitation and quenching varies with distance from the surface of the SPP supporting object. Therefore, only studies with both sufficient resolution and range see both quenching and excitation. Anger *et. al*, in 2006, were the first to experimentally observe the transition from more quenching to more excitation as it occurred, yet no-one has been able to make conclusive observations. The instrument described in this thesis is designed to make more conclusive measurements of SPPs interacting with fluorescent objects. For that reason, initial forays into studying fluorescence with the instrument are included in this thesis (see sections 3.2 & 4.3.)

1.3 Total internal reflection

The instrument described in this thesis uses total internal reflection microscopy as a primary optical tool for observing SPPs, fluorescent objects, and other objects of interest. Total internal reflection (TIR) occurs when propagating light encounters an abrupt change from high to low index of refraction and is reflected off of the interface between materials of different indices. This only occurs when the light approaches the interface from an angle steeper than or equal to a critical angle that depends on the ratio of the materials' indices of refraction: $\theta_c = \arcsin(n_2/n_1)$. See Harrick [9] or Hirschfield [11] for a more detailed discussion of why this occurs.

Though a totally internally reflected ray of light is reflected back from the interface, there is some extent to which the photons penetrate into the low index medium. This extent is localized at the surface; it does not propagate away into the far field (much like the trapped light in the polariton, but the similarity ends there.) The region of extent into the low index medium is called the evanescent field, and it is this field that is used to illuminate objects in total internal reflection microscopy.

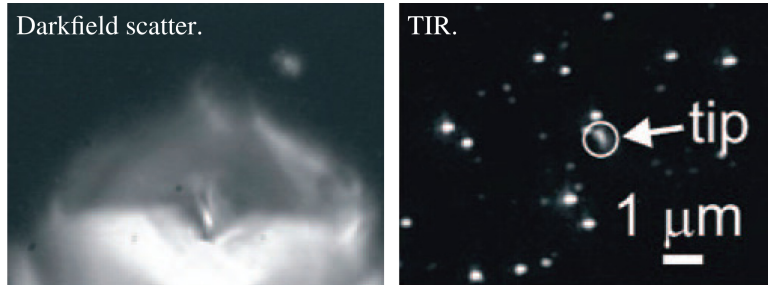


Figure 1.1: Comparison between two TIR and a more traditional darkfield microscopy technique. TIR has much greater resolution for nano-objects under the tip of the AFM. Image from [22]

Creating, imaging and measuring light scattering spectra of SPPs is a technical challenge. It is difficult to excite SPPs with conventional optical systems (see 2.1.1 for further explanation), and traditional optics are not convenient for imaging SPPs that are already excited through other means. Traditional optics collect an image from a plane of focus, but also collect out of focus ‘noise’ from objects above and below that plane. In TIR, image is only collected at and very near the interface of a high and low index of refraction material, within the extent of the evanescent field (see 2.2.5 for more).

Illuminating only this thin plane cuts down on out-of-focus background and allows for better excitation of SPPs.

1.4 Atomic force microscopy

Atomic force microscopy (AFM), sometimes called scanning force microscopy, is one of the standard tools of nanotechnology. It is a member of a wider class of instruments called scanning probe microscopes. An AFM constructs a three dimensional topograph of a surface with very high resolution (fractions of a nanometer.) To do this, the AFM pokes around with an atomically sharp tip attached to a bendable cantilever. As the tip encounters forces, the cantilever it is attached to is bent as in figure 1.2. This bending is measured by the deflection of a laser beam bounced off the back of the cantilever. By using piezoelectric materials to scan the surface of a sample in a raster pattern, a computer attached to a atomic force microscope can construct a topograph of the nanoenvioronment.

For the purposes of a plasmon polariton-associated electro-magnetic field, the atomic force microscope is a versatile tool. The ability to move the tip controllably is good for constructing topographs, but it also has a lot of potential as an avenue for manipulating the nanoenvironment. For example, an AFM can be used to align nanostructures in a specific pattern, altering the plasmon polaritons in each nanostructure by coupling the excitations together. This kind of coupling is crucial to plasmonic circuitry and enhanced optical effects that give SPPs their promise.

1.5 Our instrument

The instrument designed and constructed by our group combines total internal reflection microscopy and atomic force microscopy by literally stacking the two instruments on top of each other (see figure 1.3). This stacked configuration allows for both types of investigation at once. We are able to run the AFM and manipulate particles while recording images and spectra with the total internal reflection objective, being able to manipulate, measure, and image surface plasmon polariton supporting objects at the same time.

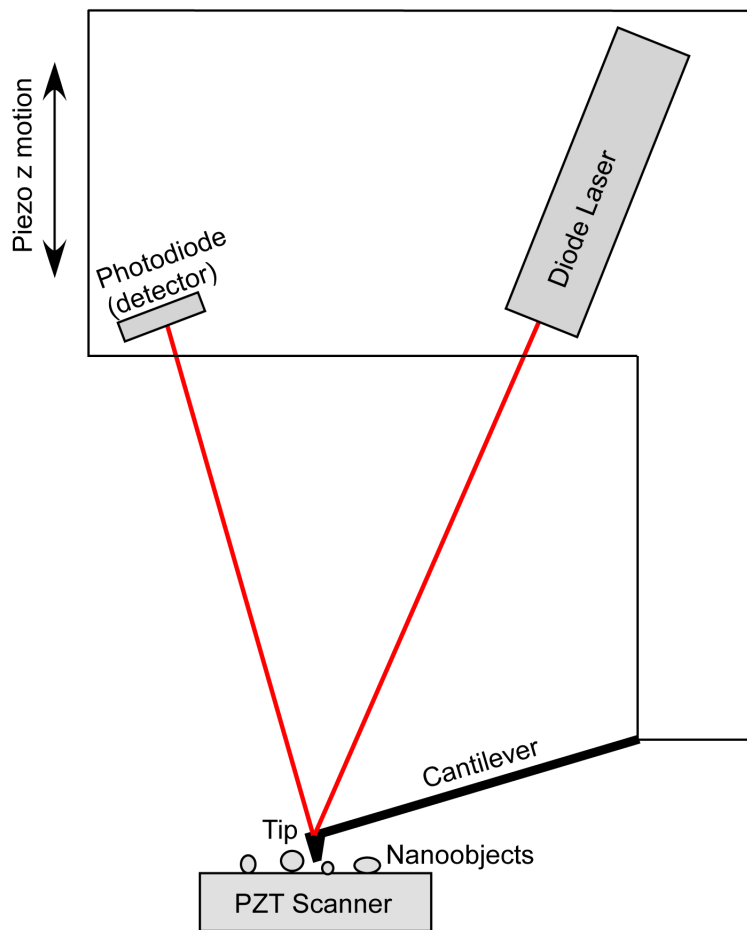


Figure 1.2: Simplified diagram of an atomic force microscope. Cantilever scans over the surface of the objects in a raster pattern, and bends. The extent of the bending is measured by change in laser position on the photodiode.

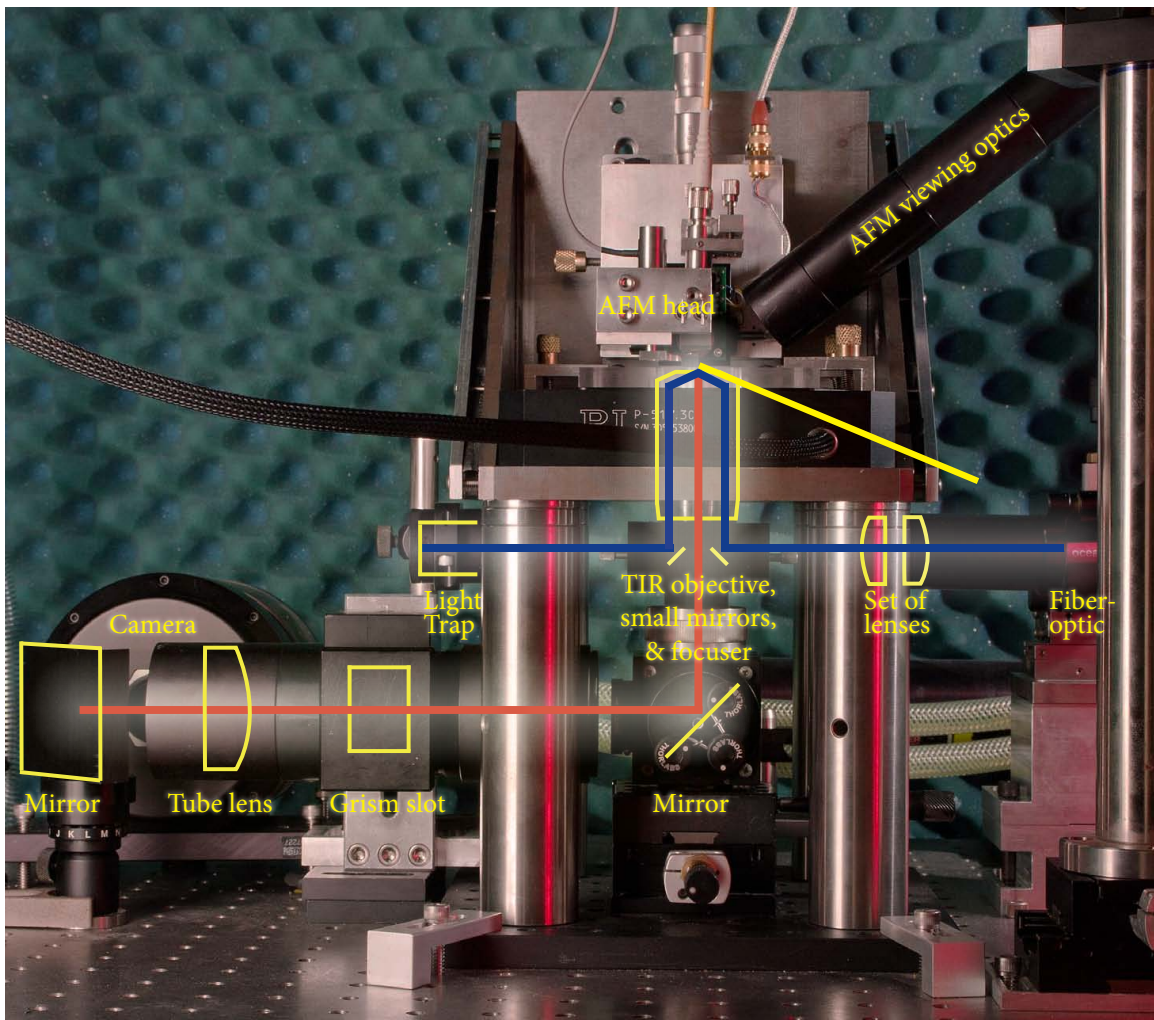


Figure 1.3: Combined atomic force/total internal reflection microscope. AFM, camera, grism, tube lens, TIR objective, and fiberoptic source are labeled. The blue line corresponds to the totally reflected beam, while the red line corresponds to one possible scattered light path.

Chapter 2

Background

2.1 Plasmons

2.1.1 Introduction; the surface plasmon polariton (SPP)

A plasmon is collective oscillation of conduction electrons in a conductor: a longitudinal wave of electron density. Surface plasmon polaritons (SPPs) involve a special case of plasmons where the oscillating electron density wave is confined to the surface of the metal, where the wave encounters a dielectric (non conducting) medium. The profile of the electron density wave at this flat surface is analogous to waves on the surface of a pond after a pebble is dropped in.

A plasmon is never static. A surface plasmon evolves along the conducting/dielectric interface. The electrons themselves may not translate appreciably through the solid, but the electron density wave does move along the surface. Even standing plasmon waves, which do not propagate along interfaces, are constantly changing in phase.

For plasmon-polaritons, the wave of high and low electron density (the plasmon) is associated with a strong electromagnetic field (the polariton). This electro-magnetic field is localized in that decays exponentially with increasing distance from the electron density wave at the interface. The small volume and high strength of the polariton is unusual. It is partially the strength and detail of SPP associated electro-magnetic fields, combined with the propagating dynamic nature of the electron density wave, that puts SPPs in a position to revolutionize so many applications.

Another fundamental application type involves surface plasmons as photon ‘traps’. As a photon excites the surface plasmon, its frequency is maintained at the plasmon frequency. In a sense, the photons are confined to

the (very small) volume of the polariton. This volume is smaller than the half wavelength of the photon, and therefore un-resolvable with traditional optics. Once trapped, the photon can travel along the surface of the metal as the electron density propagates. Proposed applications that include surface plasmons often capitalize on this potential to trap photons in small volumes and guide them controllably.

Figure 2.1 depicts a cross section of an infinite surface plasmon polariton. The electron density wave (by way of the charge distribution) the and associated electro-magnetic field of a surface plasmon polariton are both shown. The electro-magnetic field extends into both the dielectric medium and the

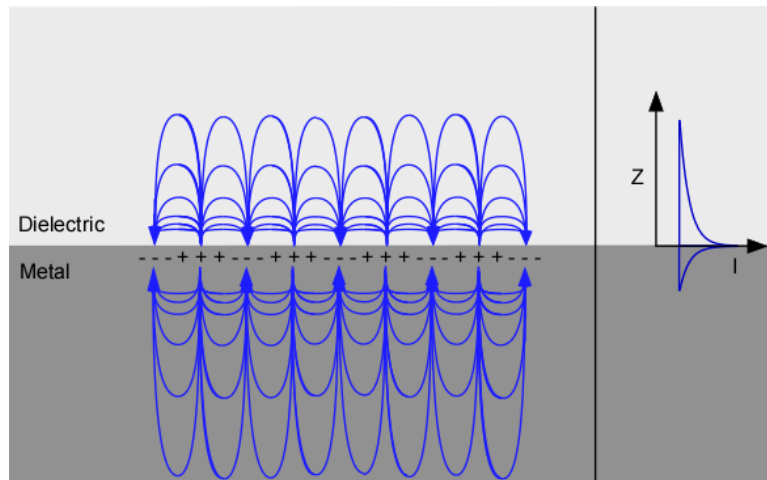


Figure 2.1: A surface plasmon polariton, with associated electro-magnetic field lines in blue. The right hand diagram represents electro-magnetic field intensity (I) *vs.* distance from the dielectric-metal interface (z).

metal, decaying exponentially with increased distance from the interface. It drops off more rapidly into the metal than into the dielectric due to the differences in electromagnetic permitivity between the materials.

Excitation of surface plasmon-polaritons using photons requires certain conditions. A photon traveling through a vacuum before hitting a flat metal surface cannot excite a SPP because doing so would violate the conservation laws of energy and momentum. Excitation can be achieved by either sending the photon through a high index medium before allowing it to hit the metal, or by creating imperfections or regular defects in the metal surface. Understanding why these conditions allow plasmon excitation to occur

requires a discussion of the relationship between energy and momentum for SPPs and the photons that excite them: their dispersion relations.

The dispersion relation

The conditions under which SPPs are allowed to form are most elegantly described through the concept of dispersion. Dispersion, generally, is any physical situation in which the velocity of an object or a set of objects is related to the energy those objects posses. Optical dispersion occurs when photons of different frequency (energy) travel at different velocities through a high index medium. Oftentimes this is coupled into a velocity dependent bending, leading to (for visible light) the creation of a rainbow. Dispersion is usually graphed in terms of angular frequency ω , phase velocity v and wavevector $k = \omega/v$. It is helpful to realize that the sign and degree of the relationships between ω and k are the same as for energy and momentum. The relationship between ω and k for any wave can be calculated from the energy and the momentum of that wave. Equations 2.1 through 2.3 derive the relationship for a photon. ($|k| \equiv 2\pi/\lambda$, where $v \equiv$ the speed of light in the medium being considered and $\lambda \equiv$ the wavelength of the same photon.) The expressions for the energy of a photon

$$E_{\text{photon}} = \frac{hv}{\lambda} = \hbar\omega \quad (2.1)$$

and the momentum of a photon

$$p_{\text{photon}} = \frac{h}{\lambda} = \hbar k \quad (2.2)$$

can be combined to give an expression for the dispersion of a photon

$$\nu\hbar k = \hbar\omega$$

more conveniently written

$$\omega = \nu k \quad (2.3)$$

In a non dispersive medium, the dispersion relation of a photon is linear ($\omega(k)$ and $E(p)$ are linear), and dependent only on the velocity of the photon.

For surface plasmon-polaritons, the dispersion relation is considerably more complex. Equations 2.4 through 2.5 derive the relationship between ω and k for an electro-magnetic wave confined to a metal/dielectric interface, including SPPs. ε_1 and ε_2 are to the dielectric functions of the two materials

[19] ($|\varepsilon_2| > \varepsilon_1$, $(\varepsilon_2 < 0)$). The magnitude of the electric field of an electro-magnetic wave is

$$E = E_0 \exp i(k_x x + k_z Z - \omega t) \quad (2.4)$$

given the boundary conditions imposed by the interface ($c \equiv 3 \times 10^8$ meters per second, the speed of electro-magnetic radiation in a vacuum).

$$\begin{aligned} \frac{k_{z1}}{\varepsilon_1} + \frac{k_{z2}}{\varepsilon_2} &= 0 \\ k_x^2 + k_{zi}^2 &= \varepsilon_1 \left(\frac{\omega}{c}\right)^2 i = 1, 2 \end{aligned}$$

gives the solution

$$k_x = \left(\frac{\omega}{c}\right) \sqrt{\frac{\varepsilon_1 \varepsilon_2}{\varepsilon_1 + \varepsilon_2}} \quad (2.5)$$

to Maxwell's equations.

An allowed excitation, (one that conserves energy and momentum) is a solution that equation 2.3 and equation 2.5 share. Graphically, this corresponds to an intercept. Figure 2.2 shows the dispersion relation for a surface plasmon in silver, and for a photon traveling through vacuum. Notice that there is no intercept (save for the physically meaningless zero energy situation); demonstrating that this excitation is impossible. The dispersion relation of either the photon or the SPP must be changed to create a situation in which excitation is allowed. For photons, the dispersion relation can be altered by altering the velocity, ν , of the photon as it hits the metal surface (refer to equation 2.3.) This can be done by changing the medium that the light travels through immediately before reaching the metal. Figure 2.1.1 graphs the dispersion relation for two different scenarios: when a photon is traveling in a vacuum and in glass. Changing the dispersion relation of the SPP at a given energy is also possible, by borrowing from crystal momentum. SPP momentum can increase or decrease by any integer amount of π/a , where a is the phonon lattice distance of the metal that supports the plasmon. In essence, the SPP is picking up momentum from phonon waves in the metal. See 2.1.4 for a more. The solid lines on figure 2.1.1 show how the dispersion line changes when a SPP gives an integer number of units of momentum to phonons in silver. The places where the lines cross in figure 2.1.1 correspond to points where photons and SPPs have the same energy and momentum, allowing far field propagating photons to couple into SPPs without violating conservation laws.

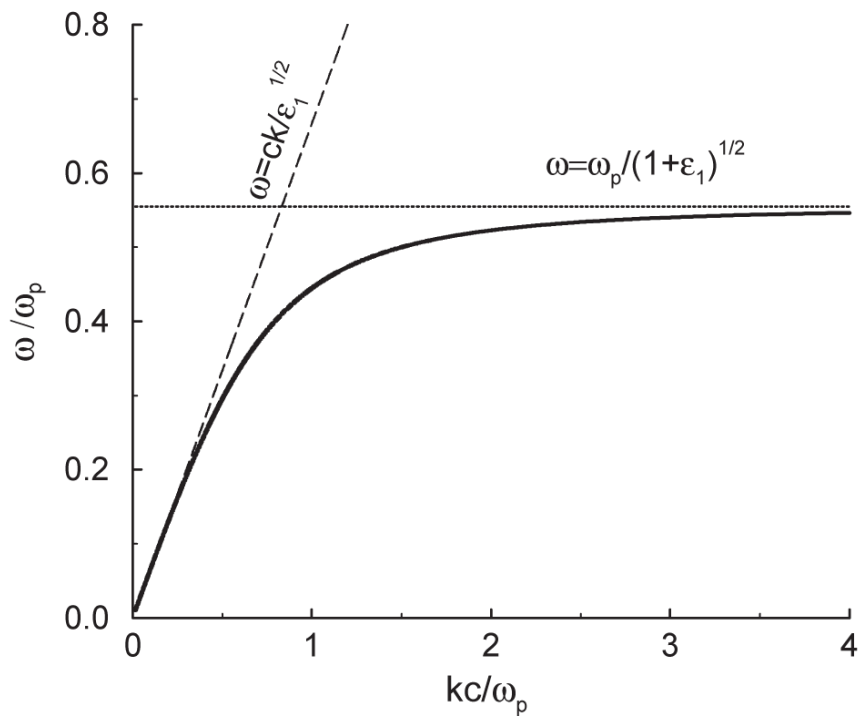


Figure 2.2: Dispersion relation for SPP in silver ($\omega_p = 11.9989 \times 10^{15} \text{s}^{-1}$) (solid line) and for light in a vacuum (line with large dashes). Also shown is the surface plasmon frequency for silver (horizontal line with small dashes). [26]

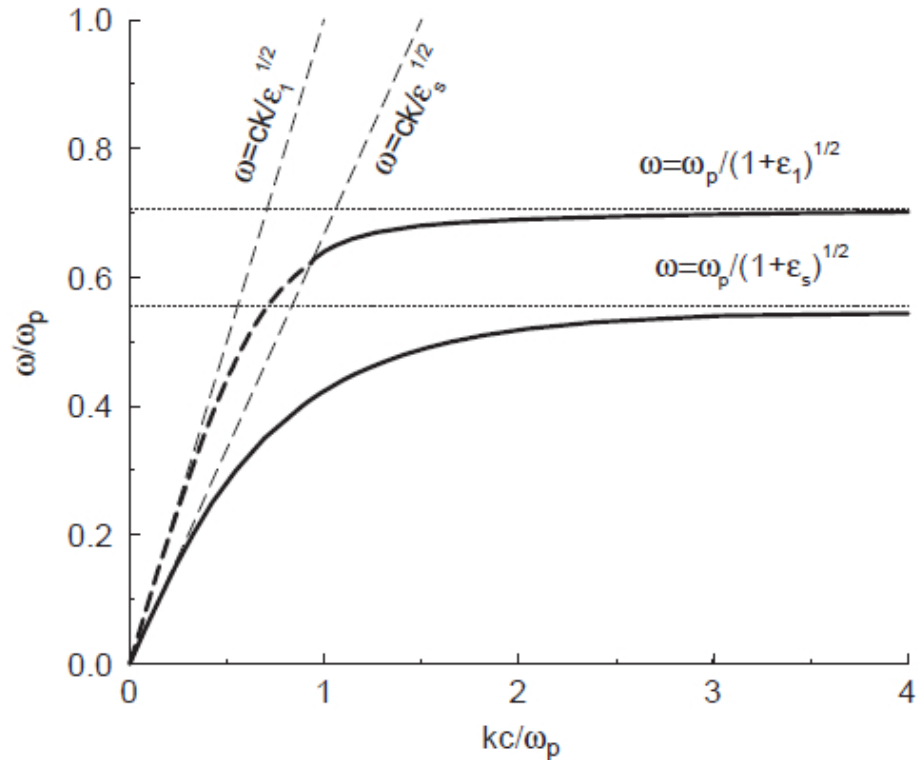


Figure 2.3: Dispersion relation for SPP in silver ($\omega_p = 11.9989 \times 10^{15} \text{s}^{-1}$) (upper solid line), silver with a change in crystal momentum (lower solid line), photons in a vacuum (left hand dashed line) and photons in glass (right hand dashed line). The locations where SPP excitation can occur have been dashed in. [26]

2.1.2 Localized surface plasmon resonance (LSPR)

An electron density wave confined to a nanoparticle rather than a surface is a localized plasmon polariton. Localized plasmon polaritons are different than SPPs in that they have specific resonance frequencies which are preferred—they exhibit enhanced plasmon amplitude at specific frequencies. These frequencies arise from boundary conditions which bound the plasmon wavefunction. A SPP supporting object will have one set of resonance frequencies for each sufficiently small dimension.

2.1.3 Plasmon-polaritons as scatterers; the spectrum of a plasmon

When a plasmon polariton supporting object exists in a oscillating electromagnetic field (it is illuminated by some light source), it can scatter into the far field. This light contains spectral information that can be used to say something about the frequency of the electron density waves in that the wavelengths of light that are absorbed by the plasmon polariton share the same frequency. Light that shares its frequency with the plasmon polariton will couple into that plasmon, and be absorbed while light that does not have a frequency that is possible to achieve with the plasmon polariton will not be as readily absorbed. The scattering spectrum of SPP supporting objects, or (especially) LSPR supporting objects tells us a lot about the energy and physical characteristics of the plasmons on that object. Optimally, one would be able to view and measure the spectrum of multiple individual plasmon supporting objects at once.

2.1.4 Crystal momentum & plasmon-polaritons

Crystal momentum is a somewhat misleading term, as a solid can possess crystal momentum even as the momentum of the crystal is zero. Crystal momentum is a term for the momentum contained in waves of excited, oscillating atoms and molecules in a lattice (phonons). The magnitude of crystal momentum is proportional to the wavelength of the phonon that makes it up – more crystal momentum corresponds to a shorter wavelength. In order to understand the physical implications of this, consider the displaced atoms that make up the phonon. Only at the location of these atoms does the phonon ‘exist’ — the movement of the atoms is the only physical manifestation of crystal momentum. The implication of this is that the crystal momentum can change by π/a without any physical change.

Crystal momentum is *not* necessarily conserved. Figure 2.4 shows the displacement of atoms in a one dimensional lattice due to two phonon waves. Though the period of the underlying phonon has changed by $2\pi/a$, the position of the atoms does not change. It is this property of being able to

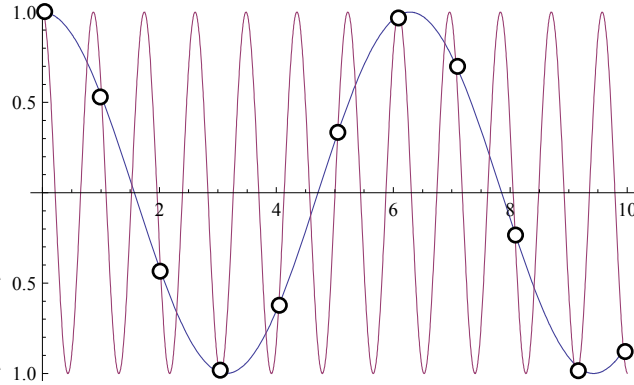


Figure 2.4: Phonons in a one dimensional lattice of atoms. Though the two phonon waves differ by $2\pi/a$, the atoms (white circles) are displaced by the same amount in both.

change phonon wavelength (and crystal momentum) without changing the physical properties of the lattices that allows SPPs to ‘freely give’ to crystal momentum, as in figure 2.1.1.

2.2 Optics

2.2.1 Index of refraction, bending light

When light passes through an interface of media with different indexes of refraction, its phase velocity changes ($v = c/n$). A medium with a high index of refraction is one where the phase velocity of light within the medium is low. When the light enters at a non-perpendicular incident angle to the interface, it experiences a change in the direction of propagation of the light, as in figure 2.5. If light moves from a high index of refraction (n_1) medium to a low index of refraction (n_2) medium its angle relative to the interface is decreased (it bends away from the vector normal to the surface). If light passes from a low index to a high index medium, its angle relative to the interface is increased. The extent to which light is bent as it passes through

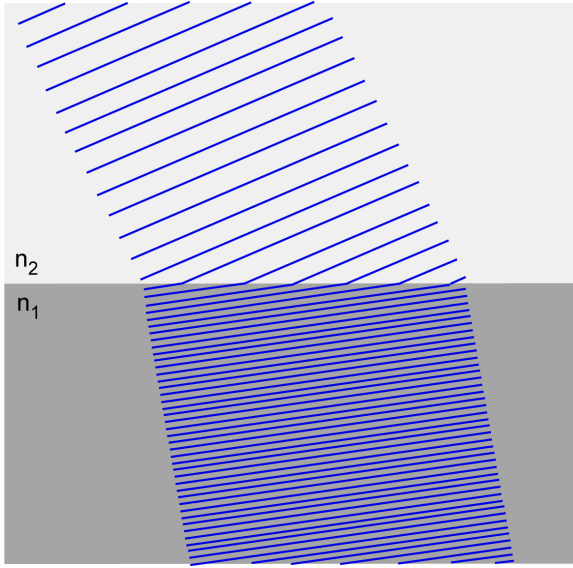


Figure 2.5: Planar light waves encountering a change in index of refraction are bent. The phase velocity and wavelength are altered, but frequency is maintained.

an interface is described by Snell's law:

$$n_1 \sin(\theta_i) = n_2 \sin(\theta_f) \quad (2.6)$$

Where θ_i and θ_f are the initial and final angles between the beam and normal. Though phase velocity is changed, the light's wavelength is decreased proportionally, so the frequency of the beam does not change over the mediums.

2.2.2 Lenses and magnification

Lenses are an application of this light bending phenomenon. Figure 2.6 is a ray tracing diagram that shows magnification due to a simple biconvex lens. The arrow in figure 2.6 points to the location where the beam is at a minimum diameter (a focus). The black lines show the edges of the beam; the beam width or spot size is the distance between the central axis and the edge of the beam. The size of the beam at this location is referred to as the beam waist. For a gaussian beam, an expression for the beam width can be written in terms of the wavelength of the beam λ , the size of the beam

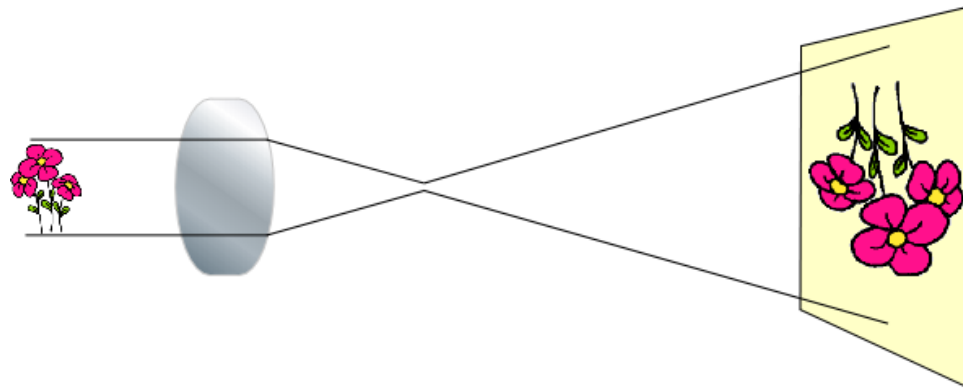


Figure 2.6: An image is magnified through a simple magnifying lens.

waist ω_0 and the distance along the central axis from the focal point z .

$$\omega(z) = \omega_0 \sqrt{1 + \left(\frac{z}{\left(\frac{\pi \omega_0^2}{\lambda} \right)} \right)^2} \quad (2.7)$$

The size of the beam waist is a function of the focal length of the lens, the beam size as it enters the lens, and the wavelength of the beam.

2.2.3 Numerical aperture, resolving power & the diffraction limit

The numerical aperture (NA) of a lens is defined as $n \sin \theta$, where n is the index of refraction of the medium outside the lens, and θ is the half angle of the cone of light that can enter the lens. The NA of a lens is inversely related by a factor to the resolving power of that lens; resolving power $\propto \lambda/NA$. Resolving power (the ability to distinguish between two points separated by distance l) has to do with the smallest imaging information that the lens can resolve. More explicitly, resolving power can be written as

$$l = 1.220 \frac{f\lambda}{d} \quad (2.8)$$

where f is the focal length of the lens, and d is the diameter of the lens. [10] There is a theoretical limit to the resolving power of traditional optical systems: the diffraction limit. For circular optics, the size of the smallest

image feature that can be resolved is called the Airy disk. This size of this disk can be approximated as

$$\sin \theta \approx 1.220 \frac{\lambda}{d} \quad (2.9)$$

where θ is in radians, and d is the diameter of the aperture.

2.2.4 Köhler illumination

The first step in imaging through any optical setup is achieving proper sample illumination. Various methods are possible, but Köhler illumination stands out because it provides even illumination with minimal alignment variables. It does this by utilizing the concept of optical fourier planes. Two planes (think of them as cross sections of the beam) in an optical path are said to be fourier planes if spatial resolution in one plane corresponds to angular resolution in the other. That means that an image at one plane (spatial resolution) will be completely unresolved in the other. By placing the sample in the fourier plane of the illumination source, Köhler illumination ensures that the sample is illuminated evenly. There is no spatial resolution at the sample and camera corresponding to source irregularities.

The TIR objective, like all lens systems, ensures that Köhler illumination occurs when an image of the illumination source (a focus of the beam) is created at the back focal plane of the objective. The set of angles that the focus entails at the back focal plane corresponds to the set of points illuminated at the sample. The more angles focused, the wider the field of view. It is therefore ideal to maximize the set of angles by maximizing the numerical aperature of the optics that focus the input onto the back focal plane of the objective. It is important to consider objects in the path of the beam that are in neither the conjugate plane of the sample nor the conjugate plane of the source. Such objects theoretically have the ability to produce resolution at the sample and camera, creating nasty background noise that ruins the experiment. The ability of these objects to do so is inversely proportional to the numerical aperture of the system; again it is beneficial to maximize input optics N.A.

2.2.5 Total internal reflection (TIR)

Total internal reflection (TIR) occurs when a beam traveling through high index of refraction (n_1) medium cannot pass into a low index of refraction (n_2) medium and instead is reflected back from the interface (internal to the

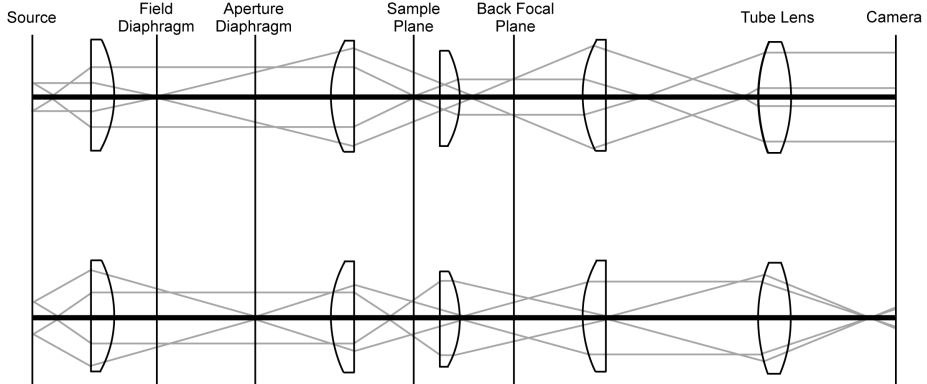


Figure 2.7: Ray tracing diagram showing Köhler illumination for a traditional (diascopic) microscope. The upper diagram shows the path of the illumination image (the so called aperture planes), the lower diagram shows the path of sample image planes. Notice that the illumination source is diffuse over the sample plane.

high index medium). This inability to pass between mediums only happens when the angle of incidence θ of the incoming light beam is less than the critical angle $\theta_c = \arcsin(n_2/n_1)$. TIR is a consequence of the way that light changes when it encounters an interface. Refer to subsection 2.2.1 and figure 2.5 for a more in depth explanation of this phenomenon.

TIR is always accompanied by an electro-magnetic field at the interface of the media, extending into but not propagating through the low index of refraction material. This electro-magnetic field is called the evanescent field, or the evanescent wave. The evanescent field decays exponentially with increasing distance from the interface. It can be most explicitly explained as a solution to Maxwell's equations for planar waves reflected off of an interface. An evanescent wave, viewed in this way, is a wavevector with at least one imaginary component. [7] Its general form would be:

$$k = e^{ikx} e^{-cx} \quad (2.10)$$

Where k and c are positive constants. This is in contrast to non-decaying waves; which have no imaginary components. Notice that equation 2.10 decays exponentially with increasing x due to the second term.

Imaging with total internal reflection

TIR imaging uses the evanescent field to illuminate objects. Since the evanescent field doesn't extend far into the low index medium, TIR imaging is a useful technique for imaging small objects at the surface of a glass coverslip (high index of refraction) and air (low index of refraction) without getting noise from out of focus objects above and below the objects of interest: TIR imaging has a very shallow depth of field. Figure 2.8 shows total internal reflection occurring at the surface of a coverslip. A single scatterer is shown within the evanescent field. The totally internally reflected light

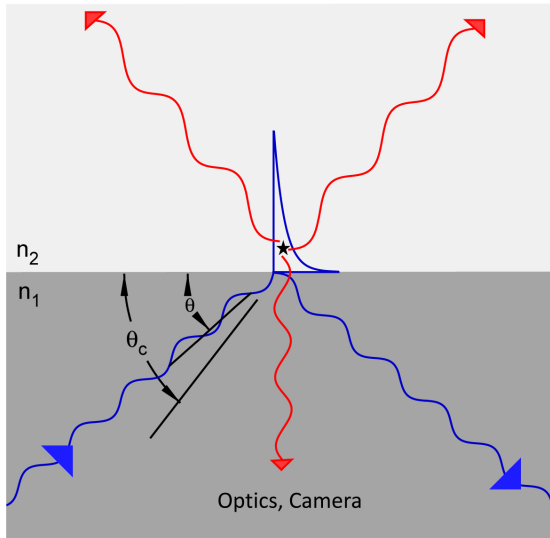


Figure 2.8: Total internal reflection. The darker material has a higher index of refraction. A single object (represented by a star) frustrates the evanescent wave and scatters light (red lines) into the far field.

is frustrated by objects at or near the surface, causing a dark object on a light background which travels down the outside of the objective. At the same time, the objects in the evanescent wave scatter light in all directions, including down the center of the objective. The objectives light collecting ability is used to the advantage of the imaging optics by placing the camera on the opposite side of the objective from the sample. In this way, the objective itself is used as an imaging lens.

Fiber optics

Fiber optic cables are a special case of total internal reflection, where light is continuously totally internally reflected through a long fiber (a ‘light pipe’). Optical fibers are distinguished by the number of possible light paths through the fiber, where cables that only have a single optical path (a single ray) are single-mode, and cables that support multiple light paths are multi-mode. Figure 2.9 shows a multi-mode fiber. Two of the modes are shown. Like lenses, fibers have a numerical aperture. In the case of fibers, the nu-

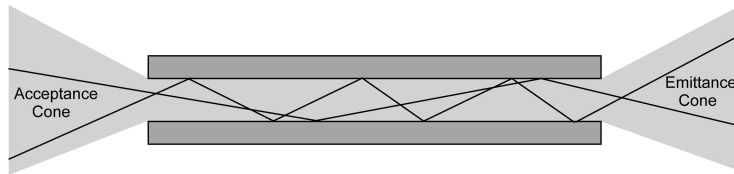


Figure 2.9: A multi-mode optical fiber, with two light paths shown.

merical aperture corresponds to the angle of the acceptance and emittance cone, as shown in figure 2.9.

2.2.6 Optical dispersion, the grism

In optics, dispersion (a frequency dependent velocity) is used to spatially separate light based on its frequency. In practice, this involves sending the light through a dispersive media to separate it into its component wavelengths.

A grism is a combination of two dispersive objects, a prism and a diffraction grating. It is used to create spectrums of multiple point sources without losing the spatial relationship between those point sources. Grisms have several inherent advantages over gratings and prisms individually. Prisms alone have wide variations in resolving power over wide spectral bands. The resolving power of a prism at any specific wavelength is a function of the prism material’s dispersion at that wavelength. The material dispersion of a prism at any specific wavelength is highly non-linear (equation 2.11)

$$\frac{\hat{\lambda}}{\Delta\lambda} = B \frac{dn}{d\lambda} \quad (2.11)$$

Gratings have a different issue. For gratings, the resolving power is wavelength independent. This means that the dynamic range of the resolving

power (the variation of the resolving power with wavelength) is fixed. Having a fixed dynamic range reduces a grating's versatility by limiting the wavelengths that it can be used with. Grisms are designed with the properties of gratings and prism in mind. Simply put, a well designed grism uses the both the tunability of prisms and the fixed properties of gratings to make an optical system with the best of both worlds (see [5] for more information.) Grisms are built to work with collimated light. In most cases the grating and the prism are physically attached, but optically this is not crucial. Refer to figure 2.10 for a simplified ray tracing diagram of a grism.

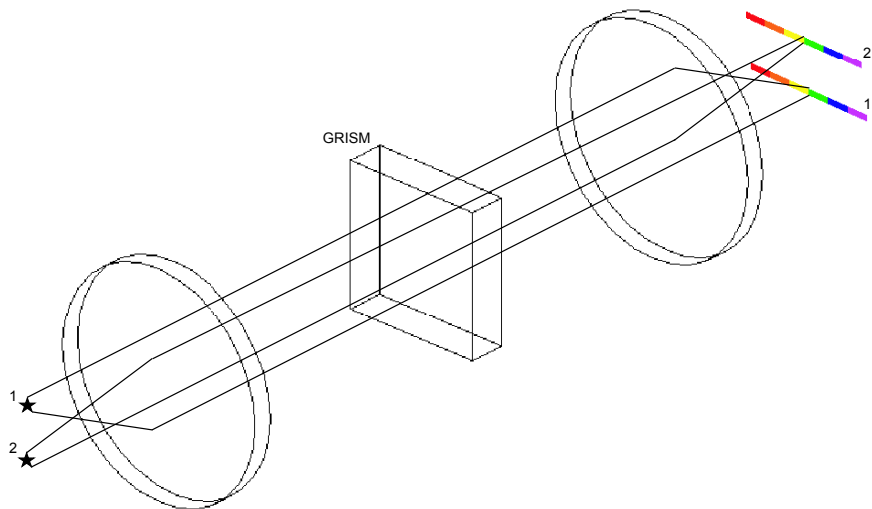


Figure 2.10: A Grism separates white light into its components. Light from scatterers in the sample plane (stars) passes through an infinity corrected lens, the grism (grating first) then a second lens focuses the light into individual spectra.

2.3 Fluorescence

Fluorescence, generally, is a process by which objects absorb light of a certain energy, lose some of that energy to vibrational states, and (except in the case of the two-photon absorption) emit a photon of lower energy (longer wavelength). Fluorescence is an important phenomenon, utilized in many scientific and industrial applications. The physical factors that govern fluorescent transitions, therefore, are of interest to scientists. The Purcell effect is of special interest because plasmon-polaritons offer an opportunity to observe the effect in new and possibly unique ways.

2.3.1 Selection rules & energy

Fluorescent transitions occur between discrete quantized energy levels. For the purposes of this discussion only electronic and vibrational energy levels will be considered, not rotational or translational. When a photon interacts with a molecule, the ability of that photon to excite electrons to higher energy state depends on certain selection rules. Essentially, these rules fall out of the universal laws of momentum and energy conservation. These rules are best understood through a grasp of symmetry and group theory as it applies to spectroscopy.

For allowed transitions, fluorescence is simply a two step process of excitation and radiative emission. There is usually an opportunity for the excited electron to relax down to a slightly lower energy via vibrational states before being emitted through so-called internal conversion. This means that fluorescent molecules often emit photons of lower energy than those they are exposed to. Spectroscopically, the difference between the excitation and emission peaks is called the Stokes shift. The fact that fluorescent objects emit light at a different wavelength than they adsorb is a unique property that can be beneficial when trying to distinguish between fluorescence and scatter.

2.3.2 Metal enhanced fluorescence & the Purcell effect

The Purcell effect states that the probabilities of fluorescent excitation or emission can each be altered by changing the electronic environment in which the fluorescent molecule resides. Specifically, Purcell showed that quantum decay (emission) differs when the emitter is placed within nanocavities of different resonant frequency. When the resonance of the cavity was in phase with the preferred resonance of the fluorescent molecule, radiative emission

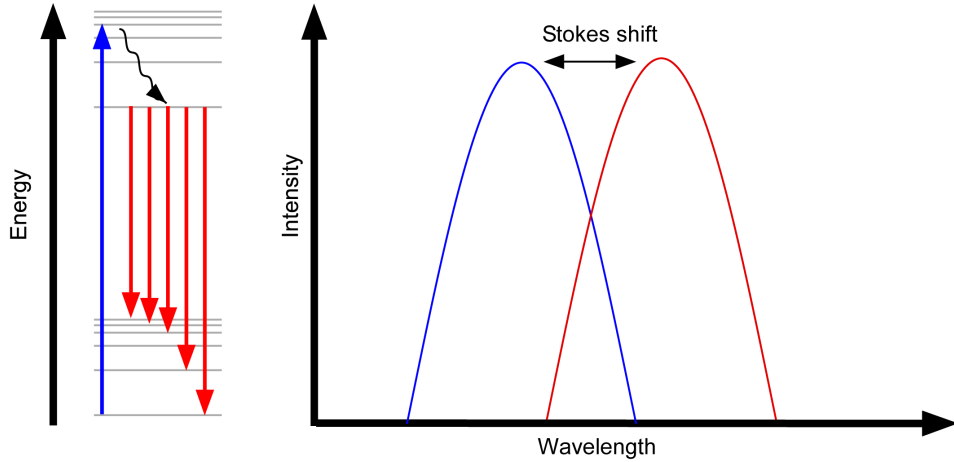


Figure 2.11: Fluorescence involves excitation (blue), internal conversion (black) and radiative emission (red). Spectroscopically, the difference in energies between the absorption (blue) and emission (red) peaks is the Stokes shift.

(as opposed to total internal decay) is increased. The rate of emission of a fluorescent object within a cavity (E_{cavity}) can be written as

$$E_{cavity} = \frac{3\lambda^3 Q}{4\pi^2 V} E_{vacuum}, \quad (2.12)$$

where V is the volume of the cavity, λ is the excitation wavelength, and Q is the so called quality factor of the cavity at the resonant mode [8]. A number of more recent studies have also reported evidence of such a relationship.

Surface plasmon-polaritons can interact with fluorescent molecules in two ways : 1) the strong electro-magnetic field can excite electrons to higher states and 2) the plasmon and associated phonons in the metal can ‘quench’ radiative decay of an excited electron by absorbing the energy in a non-radiative energy transfer. These two conflicting interactions have led to seemingly contradictory studies. Some papers report more fluorescence as molecules interact with SPPs ([20], [13]), some report less ([6], [21]), and still others report varied results ([1]). Investigating the data reveals a trend : the relative degree of excitation and quenching varies with distance from the surface of the SPP supporting object. Therefore, only studies with both sufficient resolution and range see both quenching and excitation. Studies that have sufficient resolution, however, still do not agree even on how mov-

ing fluorescent objects relative to metals affects fluorescence, much less offer up some mechanism. Anger *et. al.*, in 2006, were the first to experimentally observe the transition from more quenching to more excitation as it occurred. Further observation of metal enhanced fluorescence is one of the goals that motivated the design of this instrument.

Chapter 3

Experimental

3.1 Total internal reflection microscope

The microscope is divided into several major functional units, each of which will be discussed in greater detail in the following sections. These are the input optics, the objective and angling mirrors, and the imaging optics. Figure 3.1 shows these elements together in a simplified schematic. Totally internally reflected light (red beam) is used to illuminate the sample, while scattered light (green beam) is collected and focused into one of two CCD cameras.

3.1.1 Input optics & sources

The purpose of the input optics carriage is to produce an illuminating beam and direct it into the objective for sample illumination. It accepts a multimode fiber (400 μm diameter, Ocean Opticstm part # P400-5-VIS-NIR). The beam expands from that fiber and is quasi-collimated by an achromatic (chromatic aberration limiting) lens ($f = 45 \text{ mm}$, anti reflection coating 400 to 700 nm, Thorlabstm AC254-045-A) before being focused by another acromat ($f = 100 \text{ mm}$, anti reflection coating 400 to 700 nm, Thorlabstm AC254-100-A-ML.) Several variables need to be optimized to ensure proper TIR illumination. This discussion assumes that the beam is traveling horizontally perpendicular to the angling prism mirror and is focused correctly. Without these basic alignments, it is likely that TIR illumination will very difficult indeed.

First, the beam needs to be focused onto the back focal plane of the objective to guarantee proper Köhler illumination (see subsection 2.2.4 for more info on Köhler illumination.) For the objective used in this thesis

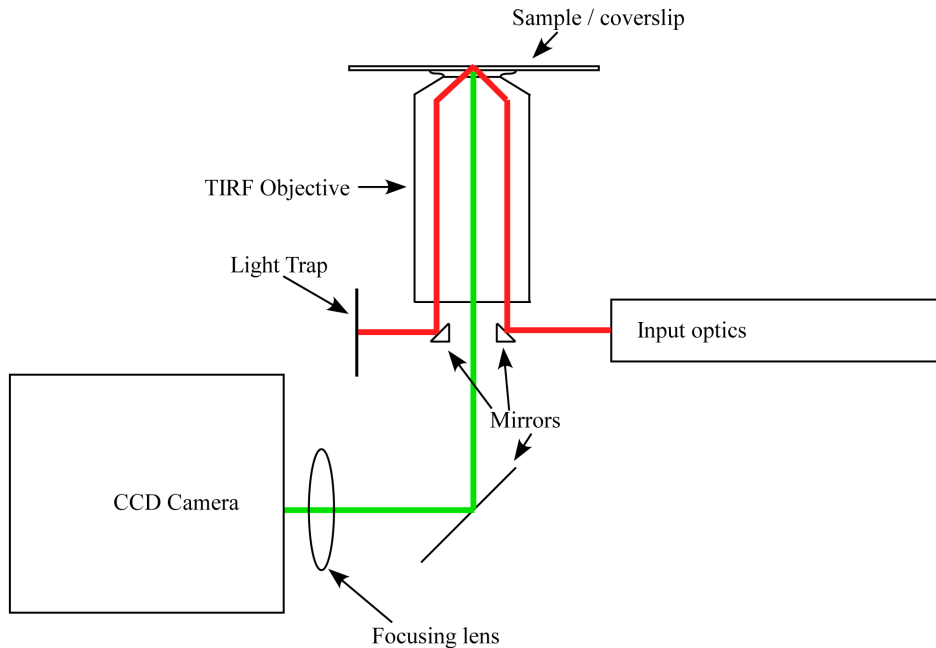


Figure 3.1: Schematic of the total internal reflection microscope. The totally internally reflected light path is shown in red, the path for scattered light is shown in green.

(Nikon CFI Apo TIRF 60x H), the back focal plane is 18.56 mm into the objective from the back face of the nose piece. To ensure that the input beam is properly focused, an alignment tool which fits into the objective slot and holds a paper screen at 18.56 mm is used. The input optics assembly is moved relative to the angling mirror until the beam is focused on the paper screen while not clipping the beam on the 5 mm angling mirror. Proper Köhler illumination ensures even illumination, but not that illumination is accomplished through proper total internal reflection.

In order to achieve total internal reflection, the focused beam at the back focal plane must be contained within the total internal reflection region. Recall that a beam is totally internally reflected back into a high index medium only when it approaches the interface at a sufficient critical angle (subsection 2.2.5.) The total internal reflection region is therefore the region where light passing through will be bent by the objective strongly enough to totally internally reflect off of the surface of the coverslip. For the Nikon

Apo TIRF 60x, this region takes the form of a ring approximately 3 mm in width at the edge of the back focal plane aperture. The focused illumination light at the back focal plane, therefore, must fit within this region. If some portion of the beam is traveling too close to the center of the objective light will be seen coming out of the sample end of the objective bent away from the input optics.

In order to achieve proper TIR without clipping the beam on the interior of the objective, move with the input angling mirror in far enough that light is seen to exit in a beam from the sample plane. Then, slowly translate the mirror towards the input optical assembly. The beam of light will be bent at a further away from the input carriage. Continue until the beam just disappears. Illuminating in this way ensures a maximum portion of the beam is used for illumination.

By ensuring that the above is true one may achieve TIR illumination. However there is one other variable of import regarding illumination; maximizing field of view by using the highest numerical aperture beam. Recall that the back focal plane is the optical fourier plane of the sample. That is to say, the set of angles at the back focal plane correspond to the set of locations at the sample plane. Ensuring that the largest possible set of angles enter the objective (having an input system with the highest possible numerical aperture) therefore maximizes the field of view.

The instrument's open design allows relatively easy changes between different modes to investigate samples in multiple ways. This is evident in the variety of light sources that have been used to illuminate samples in various experiments. In this work, the primary light source for normal white light imaging is a tungsten halogen light source from Ocean Opticstm (HL-2000-HP, 20 watt output, color temperature of 3,000 K, 360 nm - 2 μ m wavelength range.) Two lasers are available, a 632 nm helium neon laser from Xeroxtm and a 532 nm neodymium-doped doubled yttrium aluminum garnet laser (Laser Century)tm GL532RM-050FC-100-SMA-20, 50 watt output) For calibration purposes a series of atomic lamps from Electro-Technic Products, Inc. are sometimes used for their known peaks.

3.1.2 Objective, input mirrors, & sample mount

When total internal reflection occurs, the reflected beam is sent back through the objective. It exits on the opposite side of the objective, towards the side, and expands as it travels away from the objective. This beam does in fact contain information about the sample. Places where there are scattering objects on the sample plane interrupt the beam and creating dark spots;

essentially the beam is a bright-field image of the sample in the evanescent field. It may be possible to use this image in the future, but for now it is treated as ‘bad light’. It is important to position the output mirror in the correct place so that the bright-field beam is picked off completely and sent to the light trap. This can be done by translating the mirror until the beam is perfectly round and an image very bright samples can be seen.

The objective screws into a delrin box, which in turn screws into a z -translation focusing tube. Mounted into the side of the delrin box are the two 5 mm 45° prism mirrors. Each mirror is mounted on a single axis translation stage (MM3 Manual Micro-mini stage from National Aperturetm) capable of translating the mirror toward and away from the center of the box. These mirrors are mounted facing in opposite directions; one faces toward the input optical carriage (the input mirror) while the other faces a blackened tube that serves as an optical trap (the output mirror). The strength of this design is that the optics are necessarily aligned in many ways during construction. The mirrors are guaranteed to be centered relative to the objective and at the correct angle by their mounts. See the appendix for detailed drawings of the delrin box and prism-mirror mounts.

Samples are mounted on glass coverslips of thickness \approx 0.15 mm (all experiments discussed in this thesis were done on FisherFinest Premium Cover Glass.) These coverslips are placed on a Plexiglastm (poly(methyl methacrylate)) plate that accepts the objective from below and is open to the AFM above. To maximize stability, the amount of the coverslip that lies unsupported over the hole that accepts the objective is minimized. The objective-coverslip gap is bridged by type A immersion oil ($n_d = 1.515 @ 23^\circ\text{C}$) so that TIR may occur at the upper surface of the coverslip.

3.1.3 Output optics, imaging & spectroscopy

Light that is scattered by the sample passes back along the central axis of the objective and travels out the center of the back aperture, between the angling prism-mirrors, as an infinity corrected beam. This means that future lenses can be placed anywhere in the beam and still create an image of the sample. However, the further the path length between the back of the objective and the focusing lens the smaller the field of view that the lens will be able to image. When present, the grism is placed in collimated beam between the objective and the tube lens region.

There were multiple cameras used for different experiments in this work. The most commonly used camera is a Pixis 2K (2048 \times 512 imaging array with 13.5 μm square pixels, liquid cooled to -70° C), a cooled charge coupled

device (CCD) camera. The cooled CCD is very sensitive to low light levels, and is used for spectroscopy. At times, a color mosaic non cooled CCD camera is used.

Imaging

In many experimental situations, the microscope is most useful as an image taking tool. The shallow depth of field and large resolution of the TIR microscope makes it an ideal tool for imaging objects approaching the nanoscale. For imaging, the collimated beam is focused onto a camera, in most cases the cooled ccd Pixis 2K camera. in some cases, a non cooled ccd camera is used instead. This camera displays a live colored image on a tv screen. It is useful for focusing and general sample investigation, where having color and a live image is beneficial.

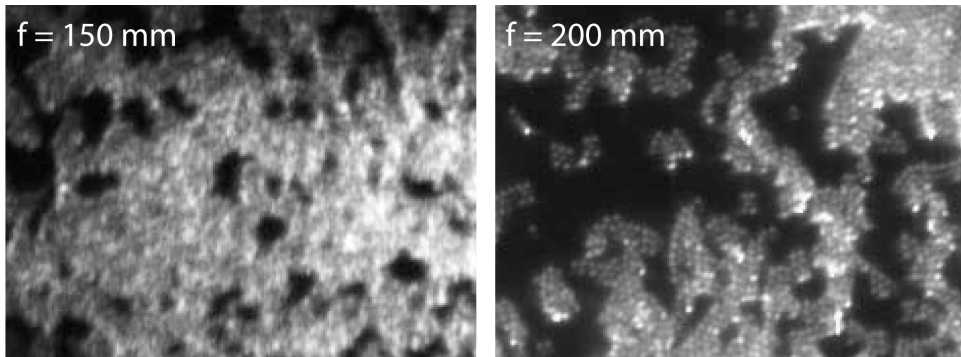


Figure 3.2: $1 \mu\text{m}$ polystyrene spheres exhibiting packing are viewed through two different tube lenses. The 200 mm tube lens is able to resolve the spheres better than the 150 mm tube lens.

It is possible to replace the last focusing lens (the tube lens) with another having a different focal length. Doing so changes the magnification of the microscope. A lens with a longer focal length yields a higher magnification. Camera-pixel limited resolution is also increased (figure 3.2), but a smaller field of view (figure 3.3.)

Spectroscopy & calibration

Spectroscopic investigations offer unique insight into plasmon-polaritons and fluorescence. Measuring scattering or fluorescence spectra is a critical func-

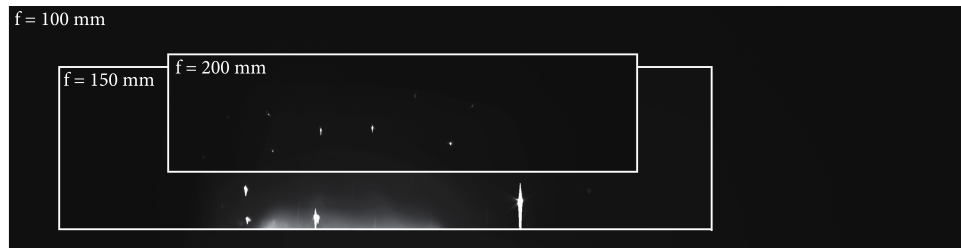


Figure 3.3: The field of view for tube lenses with different focal lengths. Tube lenses with a longer focal lengths have smaller fields of view, meaning less of the sample can be seen at any one time by the camera.

tion of the instrument. Spectra are measured with the grism placed into the path of the beam somewhere in the collimated region between the objective and the tube lens with the grating towards the objective and the prism towards the camera. The grism must be oriented so that the spectra lay along the length of the camera. The instrument has a delrin box that has a tight hole that accepts the grism with the same orientation every time. Once placed, the grism should be returned to the same location each time or the size of the spectra will change. The farther away the grism is from the objective, the larger the spectra will get at the camera.

To spectroscopically calibrate the instrument is to illuminate white point like scatterers with photons of known wavelengths, observe the peaks that are produced, and create an equation relating pixels to wavelength. The preferred method is to illuminate polystyrene spheres with atomic lamps with known emission wavelengths. Because polystyrene spheres are good scatters for every wavelength in the visible range, each will scatter the atomic spectrum when illuminated with the atomic lamp. Including emission lines from several atomic lamps, one can find the relationship between pixel number and wavelength.

Similar tube lens considerations must be taken into account when measuring spectra as were discussed earlier in regards to imaging. Tube lenses with a larger focal length will see less of the wavelength range for any one scatterer. There will again be a corresponding increase in the resolution.

When attempting to measure the spectrum of a sample, it is necessary to isolate point-like sources so that the grism may produce a clean spectrum from each source. There is no slit integrated into the optics while spectra are being measured, and the spectra of objects can overlap. Sometimes this is

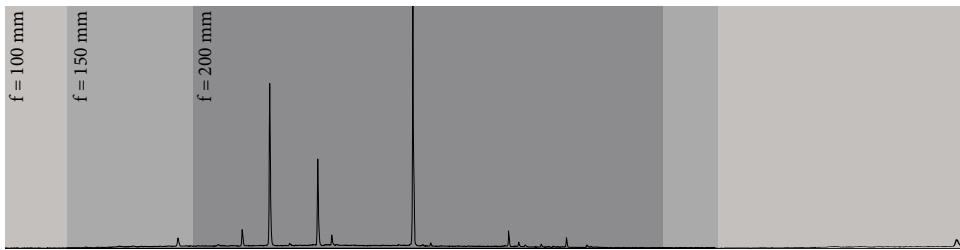


Figure 3.4: Light from a polystyrene sphere scattering He atomic lamp light is passed through the grism and viewed with different tube lenses. Tube lenses with a larger focal length are able to view a larger portion of the spectrum.

impossible due to the nature of the sample. In those situations, it is possible to illuminate only a small spot on the sample and use the grism to take a spectrum of that spot.

Creating a small spot of illumination at the sample, from a Fourier perspective, means sending light into the objective at only one angle. The easiest way to do this is to send a collimated beam into the back of the objective. An optical carriage exists to do this. It accepts the same fiber, collimates the beam with an Olympustm micro-fiche lens ($f = 52.48 \text{ mm}$, $N = 6.22$), and clips the beam to the correct size with an aperture before sending it through the objective off of the same input mirror as used for normal Köhler illumination. The input optics are not physically attached to the central instrument, so it is possible to change between focusing and collimating illumination carriages without altering the sample or AFM. Just as it is beneficial to maximize the total set of angles traveling into the back of the objective under normal illumination conditions, it is beneficial (minimizes spot size leading to the cleanest spectrum) to send a large beam into the objective in spot illumination mode. Filling the back focal plane of the objective fully with photons traveling in the same direction results in the maximum position specificity at the sample plane (see subsection 2.2.4.)

3.1.4 Improving image quality and the signal to noise ratio

Building a microscope from scratch with an open design clearly offers many benefits for experimental flexibility, but having an open design can also lead to some frustrating problems. A system such as the TIR microscope is very sensitive to any misalignment or light leakage. One of the main day

to day activities is identifying and troubleshooting the cause of background noise that obscure images and spectra. Several optical parameters (often, a combination of multiple variables) can lead to background light. These include outside light, optical misalignment, and dirty optics. The first two problems can be fixed with careful instrument assembly and screening.

Dirty optics is often the most confusing cause of background light. Scatterers on any optical surface look like out of focus noise in images. Often the amount and shape of the background noises other variables are changed in an attempt to obtain TIR, so much so that it can appear that it is in fact improper illumination that is causing background noise. Once it is determined that unclean optics are indeed the cause of background light, careful removal and cleaning of optical elements is called for. Cleaning all the surfaces is recommended; usually no surface is the sole cause of background light (see figure 3.5.) Optics should be treated very delicately. Gloves should be worn at all times, as oil from skin can ruin optical coatings. Lenses should be cleaned with lens cleaner and lens cleaning tissue in light circular motions. Front faced mirrors should be cleaned with very pure ethanol by pulling a wet lens cleaning tissue over the mirror surface gently followed by a dry tissue. The best strategy for cleaning optics is to protect optics so they don't become dirty in the first place. To clean the end of a fiber optic cable, view



Figure 3.5: Image quality improves as optics are cleaned. Each surface cleaned leads to improvement at the image, no one surface is completely responsible for background light. Sample is dust, exposures are 200 ms

the end through a fiber microscope and clean with a fiber cleaning kit. The optical fibers used in this work were cleaned with the cleanstixxtm system from MicroCare Corp.

3.1.5 Integration with AFM

Several constraints and necessary additions to the microscope exist due to the integrated AFM system. First, the microscope has to be very stable and vibrations must be minimized to avoid introducing noise into the AFM signal. Sturdy posts and vibration isolation mounting does a lot to accomplish this. Since the TIRF objective is of the oil immersion type and the sample must be mounted on a very thin glass coverslip, any instability in the objective relative to the AFM and sample can couple vibrations into the sample and AFM system reducing the resolution until the AFM is unusable. The cooled camera uses a mechanical shutter which creates vibrations when it is opened or closed electronically. To minimize the effect of this vibration on the AFM the camera rests on feet of absorbing vibration absorbing material.

The microscope needs the ability to move millimeters relative to the sample/AFM to account for variability in tip placement. To accomplish this movement two translation stages, stacked perpendicular to each-other, exist between the objective/delrin box/prism mirror assembly and the breadboard. The tip may be found by using these translation stages to move the objective relative to the AFM. In this work, the tip was typically found by moving the laser off the front of the tip while the AFM was not in contact, then slowly translating the TIR objective until the laser entered the objective and exited the tube lens. Then, the laser beam was slowly returned its correct position while the objective was translated to maintain the laser spot after the tube lens. Once the laser is again bouncing off of the back of the cantilever the form of the cantilever will likely be seen in relief as in figure 4.1. Move the tip into contact with the sample to view its location exactly as illuminated via TIR.

3.2 Fluorescence investigations

3.2.1 Fluorescent nanospheres

Fluorescent nanospheres (2.5% solids, TransFluoSpheres, Invitrogen, 633/720, T8870) were diluted 1:500 times and spin coated onto a coverslip at 5000 rpm for 30 seconds.

3.2.2 Dye coated surface

Surfaces evenly coated with dye are of interest as potential tools for metal-enhanced fluorescence observation. After a period of development, a procedure was found to yield a surface with even fluorescence over large regions [15]. Brilliant cresyl blue dye in 2% 950 K PMMA was dissolved in chlorobenzene (MicroChem) to a concentration of 5×10^{-2} M. The resulting solution was stirred overnight, then spun in a microcentrifuge for 5 minutes at top speed to remove undissolved dye. The resulting supernatant was drawn off and diluted 10-fold to a concentration of approximately 5×10^{-3} M in PMMA/chlorobenzene. $500 \mu\text{L}$ of the resulting was spin coated onto solution onto a coverslip at 800 rpm for 1 minute.

3.3 Plasmonic investigations

3.3.1 UV-Vis absorption spectra of gold nanorods

Uncoated gold nanorods were purchased from Nanopartztm. Nanorods of four lengths were purchased: 34, 47, 60 and 73 nm. All rods had a diameter of 25 nm, and were shipped in deionized water with < 0.1% ascorbic acid and < 0.1% CTAB (cetyltrimonium bromide) surfactant capping agent. $10 \mu\text{L}$ of each rod-containing solution was diluted to 1 mL with deionized water. The UV-Vis absorption spectra of the subsequent solution was taken with ..info about spectrophotometer.. Each rod solution came at a slightly different concentration from the manufacturer. Refer to table 3.3.1 for details regarding the concentration of rods in each cuvette.

Length (nm)	Axial Diameter (nm)	Reported Peak Wavelength	Nanoparticle Size mL	Moles Nanoparticles L	mg mL	ppm
34	25	550	5.2^9	3.11×10^{10}	0.911	414
47	25	600	5.2^9	3.70×10^9	1.498	681
60	25	650	2.6^9	4.55×10^{10}	2.351	1069
73	25	700	1.3^9	2.71×10^{10}	1.705	755

A scattering spectrum of all four nanorods together was also measured. $10 \mu\text{L}$ of all four rod-containing solutions (a total of $40 \mu\text{L}$) were diluted to 1 mL in deionized water. The UV-Vis absorption spectra of the subsequent solution was taken with the same spectrophotometer.

3.4 Imaging of gold nanorods

2 μL of a solution of 73 nm \times 25 nm uncoated nanorods from Nanopartztm was placed directly onto a coverslip. The nanorods were imaged within the resulting droplet of water.

3.5 Nanosphere lithography

Nanosphere lithography is a process through which packed nanospheres (1 μm spheres from Polysciences Inc.) are used as a resist template to create (in this case) a web of metal. Coverslips washed in water and ethanol were exposed to an ozone-producing UV lamp for 15 minutes. Dilute nanospheres 6:1 in spectroscopy grade methanol and were spin coated onto the coverslip at 500 rpm for 1 minute then 3000 rpm for 15 seconds. The resulting slide was sputter coated with gold/palladium at 150 millitorr and 10 milliamperes for 2 minutes. Template polystyrene spheres were removed by sonication in ethyl acetate for 45 minutes to an hour. Optionally, coat the resulting metal webbing with dye as in 3.2.2.

Chapter 4

Results & Discussion

4.1 Instrumental successes

The design and construction of the combined atomic force (AFM) / total internal reflection (TIR) microscope was carried out with specific goals in mind: TIR imaging, measuring spectra and the AFM topographs, and being able to do the above together in various combinations. This section gives highlights regarding the completion of those goals in the current iteration—it motivates the construction of the instrument and serves as a proof of concept for future work.

Producing a recognizable image of the sample is the first step in investigation of a new sample. Compared to producing spectra or AFM topographs, taking a picture is relatively simple. Still, there have been setbacks and delays in image production. Refer to the experimental chapter (sections 3.1.3 & 3.1.4) for more on these struggles. Despite struggles, successful images have been taken as seen throughout this chapter. The AFM tip has successfully been viewed through the microscope under TIR illumination—a particular challenge. In fact, gold nanorods have been manipulated using the AFM while viewed through TIR (see figure 4.1.)

Using the microscope to measure the spectrum of individual nano-objects has been considerably more difficult. Because of the nature of the grism and the quantitative nature of spectroscopy, signal to noise has been a problem. No individual surface plasmon polariton (SPP) spectrum has been taken. Still, spectra of known samples, such as atomic lamps illuminating polystyrene spheres have been taken; taking individual plasmon polariton spectra is only a matter of increasing signal to noise ratio sufficiently.

AFM topographs have been constructed successfully as well. Figure 4.2

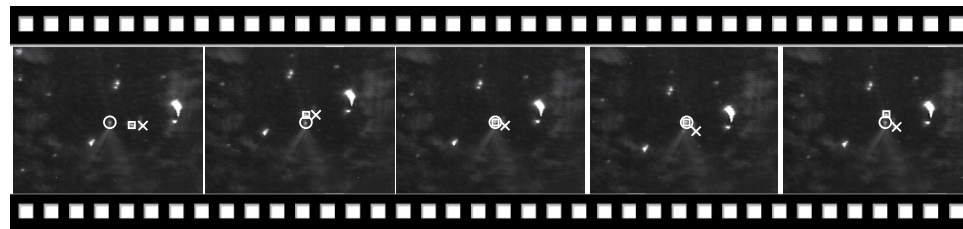


Figure 4.1: The AFM tip (circle) pushes a cluster of gold nanorods (square) relative to some reference objects (cross). The shape of the cantilever can be seen in relief of scatter from the AFM laser.

shows an AFM topograph of $1\text{ }\mu\text{m}$ polystyrene spheres next to optical images of the same sample. The irregularity in the spheres on the AFM topograph is likely due to tip defects.

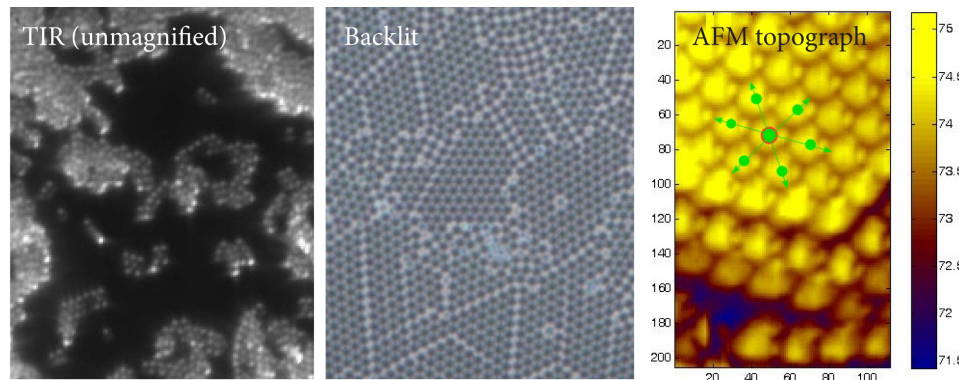


Figure 4.2: $1\text{ }\mu\text{m}$ polystyrene spheres allowed to self deposit onto a coverslip tend to pack together regularly. A sample of such packing is imaged with three instruments—the TIR microscope, the modular scope from the Bates College Imaging Center, and the AFM. Notice the lattice defects.

4.2 Plasmonic investigations

4.2.1 Imaging of gold nanorods

Gold nanorods were successfully imaged using TIR. Figure 4.3 shows the image produced when a droplet of water containing nanorods is imaged using TIR. Background light is believed to be caused by the consequences to proper TIR of imaging in a relatively high index material such as water.

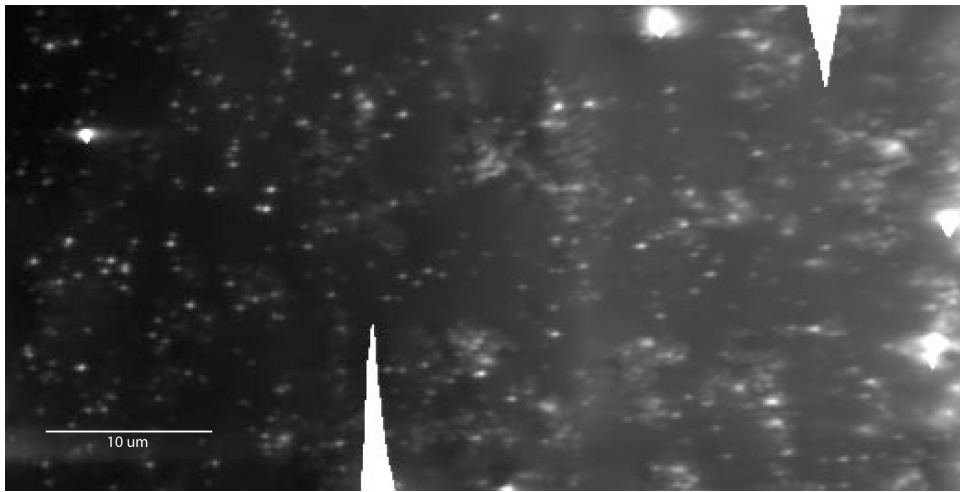


Figure 4.3: Gold nanorods in water. Some regions have deposited themselves onto the surface.

4.2.2 UV-Vis absorption spectra of gold nanorods

Recall that gold nanorods support localized surface plasmon resonance. This phenomenon causes the gold nanorods to preferentially absorb certain frequencies of light matching LSPR resonance frequencies. It is possible to observe this preferential absorption with spectrophotometry (see section 4.2.2 for details). Multiple peaks were observed for solutions of nanorods with disparate lengths and diameters, with longer rods producing peaks with longer wavelengths. Therefore, it is likely that the higher wavelength peaks correspond to photons donating into the lower frequency LSPR along the length of the nanorod, the lower wavelength peaks to LSPR across the diameter of the rod. As all four rod types were the same diameter, the radial mode LSPR is shared between the four of them.

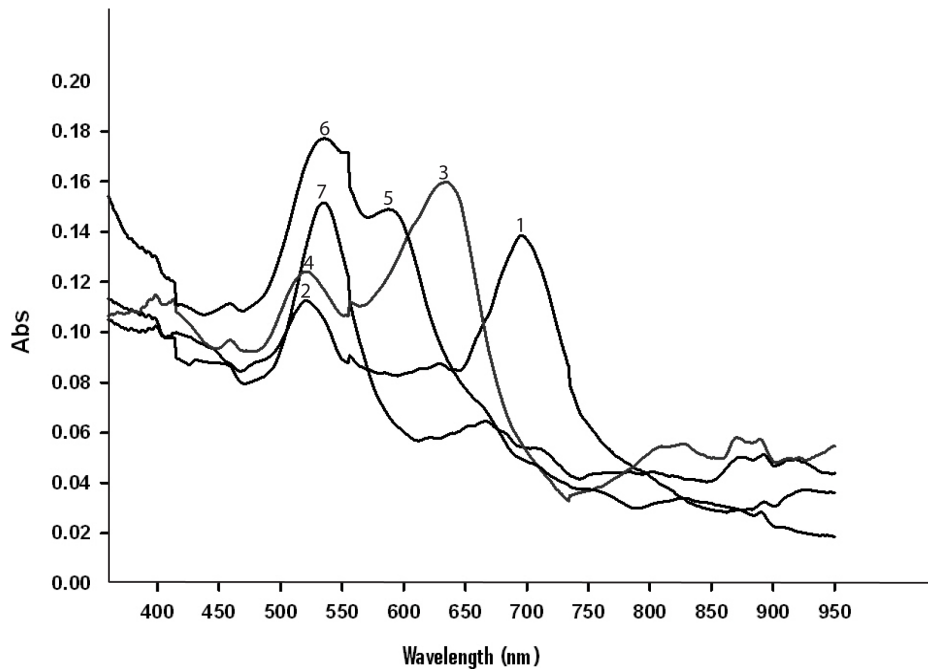


Figure 4.4: Absorbance *vs.* wavelength scattering spectra for solutions of gold nanorods. Peaks 1, 3, and 5 correspond to LSPR along the length of the nanorods, with longer nanorods absorbing at a higher wavelength. Peaks 2, 4 and 6 correspond to LSPR along the diameter of the rods, the same in all four cases. Peak 7 overlaps LSPR along dimensions in rods that have a length that approaches their diameter.

4.3 Fluorescence

Investigations into metal enhanced fluorescence are still underway. This section gives a report on progress which has been made.

4.3.1 Viewing fluorescence with TIR

To view only fluorescence, we illuminate with light of a single color. Then a filter is placed at the camera which only allows photons of longer wavelength than the illumination photons to pass through. Only photons which emanate from fluorescent transitions (and are therefore of lower energy and longer wavelength than the illumination) will therefore reach the camera and produce an image. Using this method, fluorescence was successfully

observed in fluorescent micro-spheres using TIR microscopy. See figure 4.5.

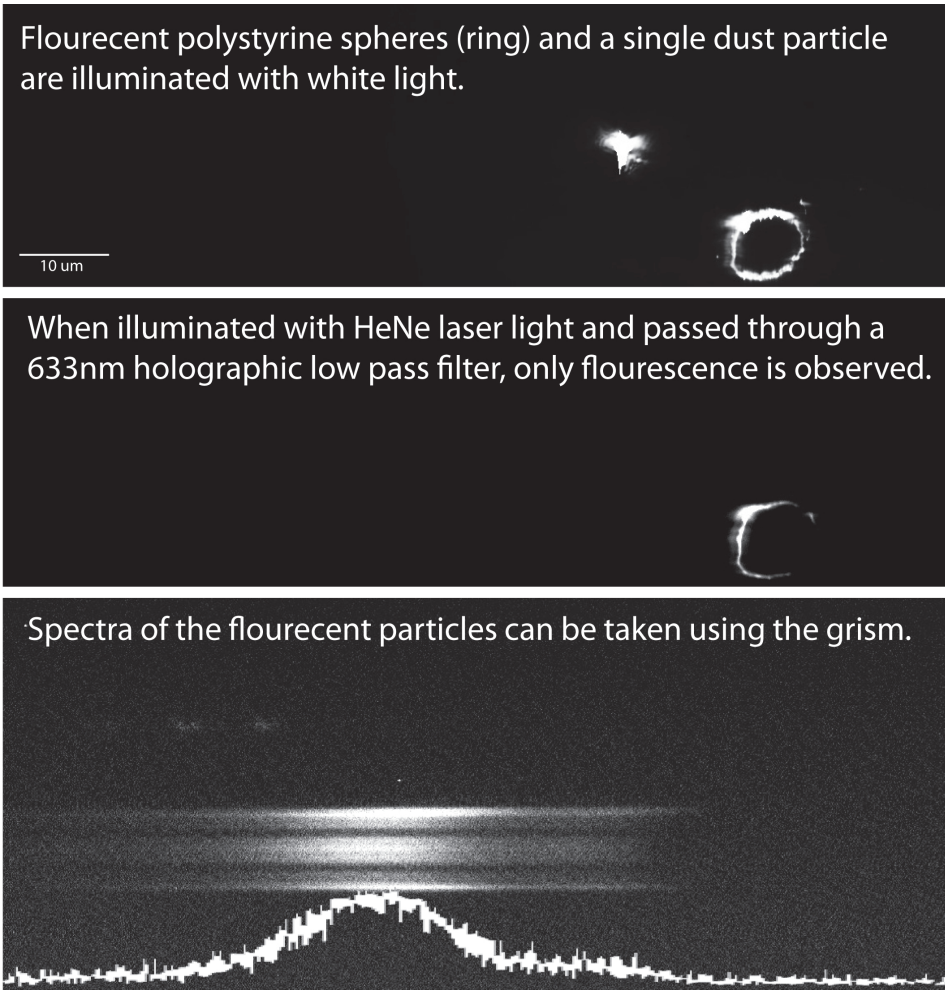


Figure 4.5: A ring of 356 nm polystyrene spheres imbued with fluorescent dye and a dust particle are viewed in three different modes. A spectrum (pixel *vs.* intensity) is shown for the grism image.

4.3.2 Cresyl-blue coated surface

Through intelligent trial and error, a procedure for coating a surface with an even coating of fluorescent cresyl-blue dye in PMMA polymer has been

developed [15]. Refer to subsection 3.2.2 for the detailed procedure. To verify that such a surface does indeed exist, collimated light was sent into the back of the TIR objective to create a small spot of illumination (as explained in subsection 3.1.3.) Illumination was accomplished with 632 nm HeNe laser light. A low pass holographic filter with a 633 nm cutoff was installed immediately before the camera to filter out scattered light so that only light from fluorescence reached the camera. Refer to figure 4.6. The

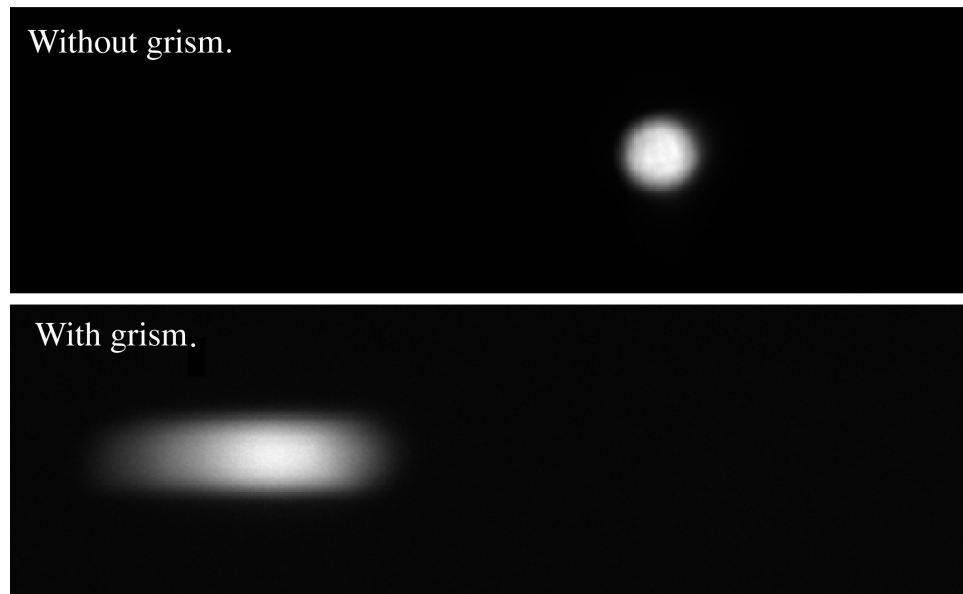


Figure 4.6: A coverslip coated in brilliant cresyl blue in PMMA/Chlorobenzene is viewed in spot spectroscopy mode. Illumination in both cases is from a HeNe laser, and in both cases a low pass holographic filter with 633 nm cutoff is installed immediate to the camera. The shape, intensity, and morphology of the spot does not change as the sample is moved. In both cases the camera shutter was open for 10 ms.

spot appears so large because of limitations in our collimated illumination strategy—the numerical aperture is limited by the size of the angling prism. The shape, intensity, and morphology of the spot does not change as the sample is moved, therefore we conclude that the the surface is indeed an even coating of fluorescent material.

4.3.3 Nanosphere lithography

The nanosphere lithography experiment was conducted in an attempt to observe metal enhanced fluorescence by observing either increased or quenched fluorescence in relation to a ordered metal lattice. The metal is laid down in a semi-regular array via deposition using polystyrene nanospheres as a template (see section 3.5 for experimental details.)

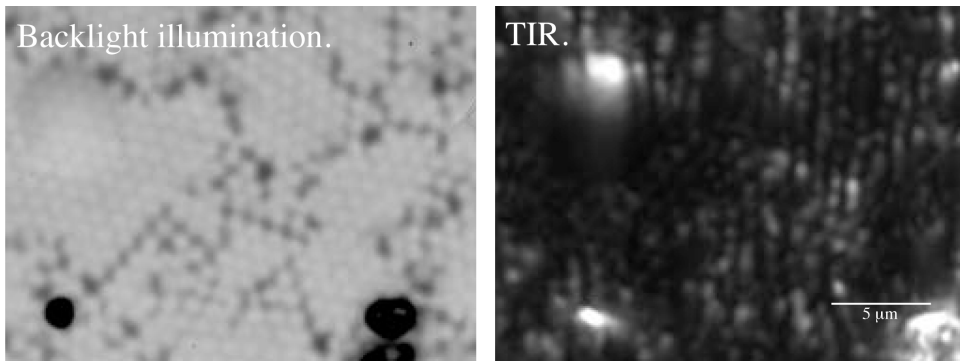


Figure 4.7: $1\text{ }\mu\text{m}$ polystyrene nanospheres are used as relief during gold sputtering, then removed. The resulting sample is a lattice of gold metal along with a fair amount of left over of polystyrene. Here, the same sample is viewed with the TIR microscope using two different illumination schemes. In the first, dark regions correspond to objects (gold or polystyrene). In the second, light regions correspond to the same objects.

Figures 4.7 and 4.8 show samples left at two stages of the lithography process. The first is after gold sputtering and nanosphere removal. The sample is a lattice of gold metal with clumps of un-removed polystyrene (from the polystyrene spheres used as a template during the lithography process) on the surface. The second is the same sample after being coated with fluorescent dye. There was no observed pattern to the fluorescence relative to the gold lattice, only fluorescent hot spots where the dye was caught in the polystyrene globs. Again, it is possible that a higher signal to noise could reveal a fluorescent response to the gold wires—further investigation is warranted.

4.4 Conclusion, looking forward

The development and construction of the combined TIR/AFM microscope was successful, and some initial forays into observing plasmonics and metal-

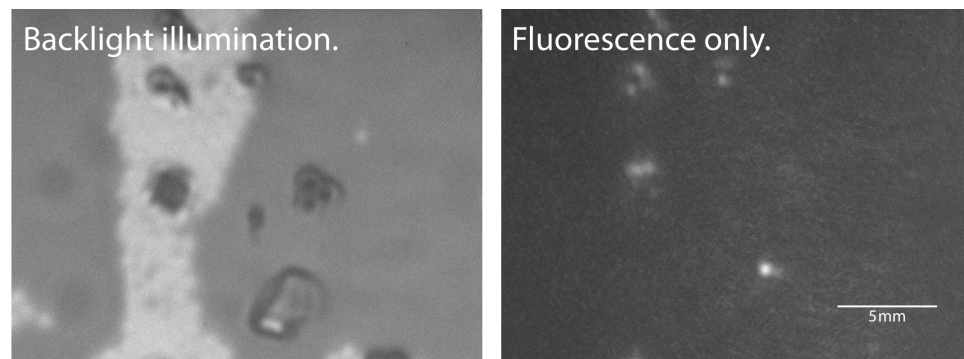


Figure 4.8: The sample in figure 4.7 was coated with cresyl-blue and viewed again. Fluorescence only illumination is accomplished through TIR as explained in subsection 4.3.2.

enhanced fluorescence serve as an excellent motivation toward further work in developing and using the instrument.

Bibliography

- [1] Anger, P.; Bharadwaj, P.; Novotny, L. Enhancement and Quenching of Single-Molecule Fluorescence. *Phys. Rev. Lett.* **2006**, *96*, 113002, 1–4
- [2] Barnes, W. L.; Dereux, A.; Ebbesen, T. W. Surface plasmon subwavelength optics *Nature* **2003**, pp 824–830
- [3] Bozhevolnyi, S. I.; Volkov, V. S.; Leosson K Localization and Waveguiding of Surface Plasmon Polaritons in Random Nanostructures. *Phys. Rev. Lett.* **2002**, *89*, 18, 18601-(1-4)
- [4] Bozhevolnyi, S. I.; Volkov, V. S.; Devaux, E.; Laluet, J-Y.; Ebbesen, T. W. Channel plasmon subwavelength waveguide components including interferometers and ring resonators. *Nature*. **2006**, *440*, 508-511
- [5] Chen, C. W.; Gossett, E. W. Grism (grating-prism combination). US Patent 5,652,681, **Jul 29, 1997**.
- [6] Dulkeith, E.; Ringler, M.; Klar, A.; Feldman, J.; Gold Nanoparticles Quench Fluorescence by Phase Induced Radiative Rate Suppression. *textit{Nano Lett.}* **2005**, *5* 585.
- [7] Felsen, L. B. Evanecent waves. *J. Opt. Soc. Am.* **1976**, pp 751-760
- [8] Gaponenko S. V.; Guzatov, D. V. Possible rationale for ultimate enhancement factor in single molecule Raman spectroscopy. *textit{Chem. Phys. Lett.}* **2010**, *477*(4-6), 411–414
- [9] Harrick, N. J.; Internal Reflection Spectroscopy. *John Wiley & Sons Inc.* **January 1967**.
- [10] Harris, J. L. Diffraction and Resolving Power. *J. Opt. A: Pure Appl. Opt.* **1964**, *54*, 7, 931–936

- [11] Hirschfield, T. Procedures for Attenuated Total Reflection Study of Extremely Small Samples. **1967**, *6*, 4, 715–718
- [12] Krasavin, A. V.; Zyats, A. V.; Zheludev, N. I. Active control of surface plasmon-polariton waves. *J. Opt. A: Pure Appl. Opt.* **2005**, *7*, S85-S89.
- [13] A. Kramer et al., *Appl. Phys. Lett.* **2002**, *80*, 1652.
- [14] Lamprecht, B.; Krenn, J. R.; Schinider, H.; Ditlbacher, M.; Salerno, N.; Felidj, A.; Leitner, F. R.; Ausseneegg; Weeber, J. C. Surface plasmon propagation in microscale metal stripes. *Appl. Phys. Lett.*, **2001**, *79*, 51 51–54
- [15] Morgan, E. Studying Plasmonic Nanostructures Using Fluorescence. *Senior Thesis, Bates College* **2011**.
- [16] Okamoto, K.; Niki, I.; Scherer, A. Surface plasmon enhanced spontaneous emission rate of InGaN/GaN quantum wells probed by time-resolved photoluminescence spectroscopy. *Appl. Phys. Lett.* **2005**, *87*.
- [17] Pitarke, J. M.; Silkin, V. M.; Chulkov, E. V.; Echenique P. M. Theory of surface plasmons and surface-plasmon polaritons. *Rep. Prog. Phys.* **2007**, *70*, 1-87.
- [18] Ritchie, R. H. Plasma Losses by Fast Electrons in Thin Films *J. Phys. Rev.* **1957**, *106*, *5*, 874-881.
- [19] Sambles, J. R.; Bradbery, G. W.; Yang, F. Optical excitation of surface plasmons: an introduction. *J. Cont. Phys.* **1991**, *32*, *3*, 173-183.
- [20] Shimizu, K. T.; Woo, W. K.; Fisher, B. R.; Eisler, H. J.; Bawendi, M. G. Surface-Enhanced Emission from Single Semiconductor Nanocrystals. *Phys. Rev. Lett.* **2002**, *89*(11), 117401/1–117401/4
- [21] Trabensinger, W.; Kramer, A.; Kreiter, M.; Hecht, B.; Wild, U. P. Single-molecule near-field optical energy transfer microscopy. *Appl. Phys. Lett.* **200**, *81*(11), 2118–2120
- [22] Sherry, L.J.; Rongchao, J.; Mirkin, C.A.; Schatz, G.C. Van Duyne, R.P. Localized Surface Plasmon Resonance Spectroscopy of Single Silver Triangular Nanoprisms *Nano Lett.* **2006**, *6* (9), 20602065
- [23] Vuckovic, J.; Loncar M.; Scherer Surface Plasmon Enhanced Light-Emitting Diode. *IEEE Journal of Quantum Elec.* **2000** *36*, *10* 1131–1144

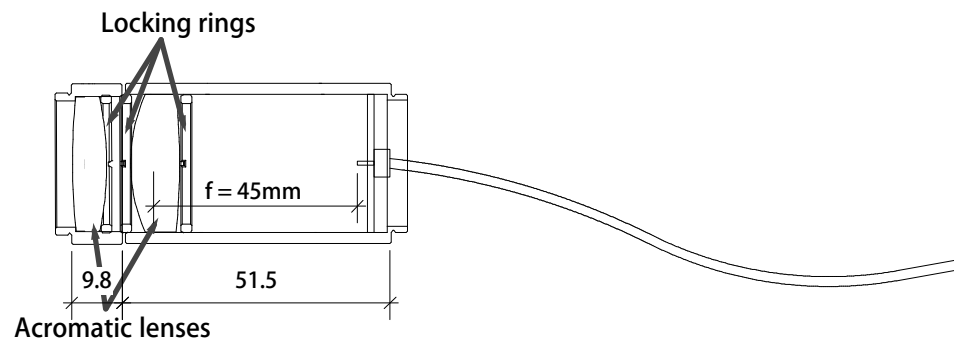
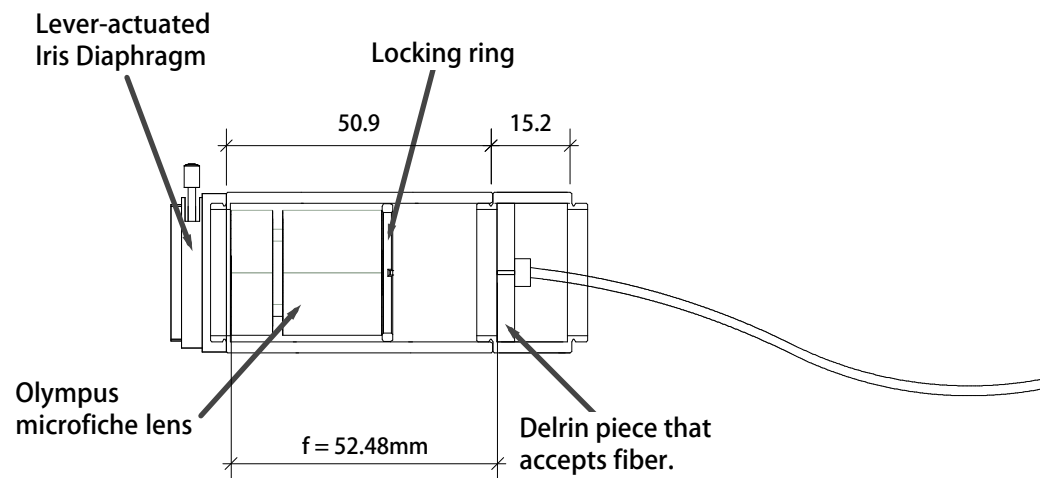
- [24] Wedge, S.; Barnes, W. Surface plasmon-polariton mediated light emission through thin metal films. *Opt. Express.* **2004**, *12*, 3673–3685
- [25] Weeber, J.-C.; Krenn, J. R.; Dereux, A.; Lamprecht, B.; Lacroute Y.; Goudonnet, J. P.; Near-field observation of surface plasmon polariton propagation on thin metal stripes. *Phys. Rev. B.* **2001**, *64*.
- [26] Zayats, A. V.; Smolyaninov I. I.; Maraddudin A. A. Nano-optics of surface plasmon polaritons. *J. Phys. Rep.* **2005**, *408*, 131–314.

Appendix A

The instrument

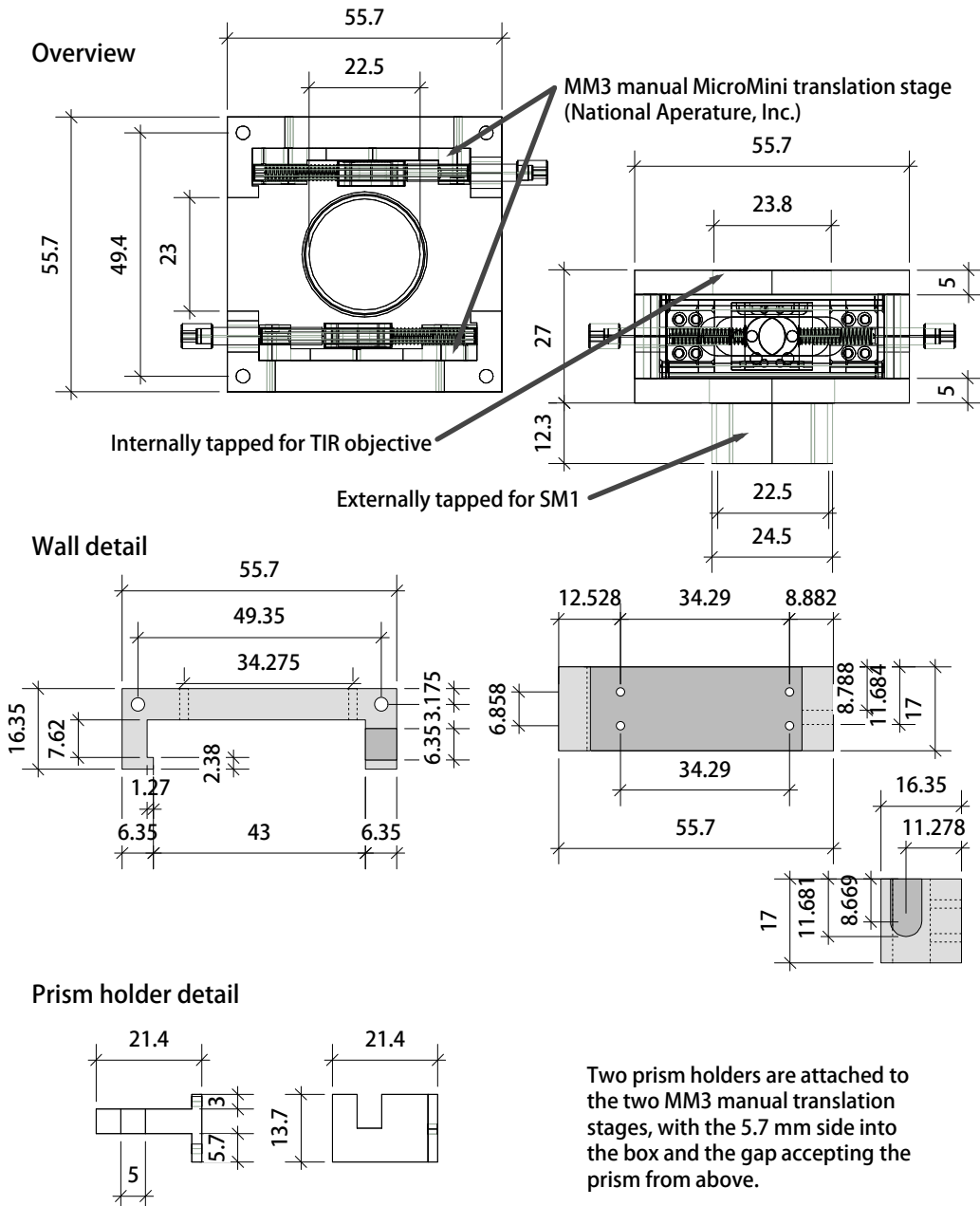
Focusing optical carriage.

To scale.

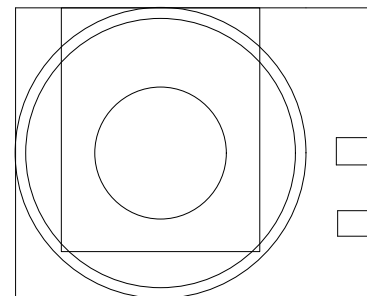
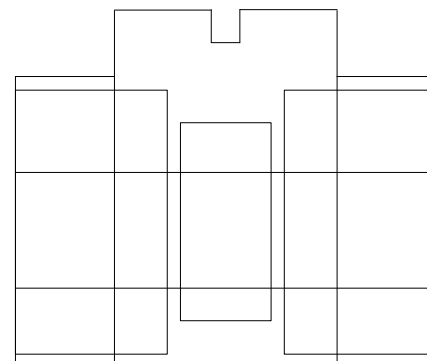
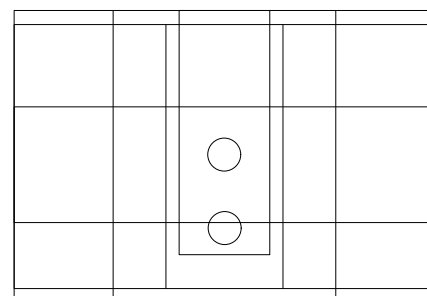
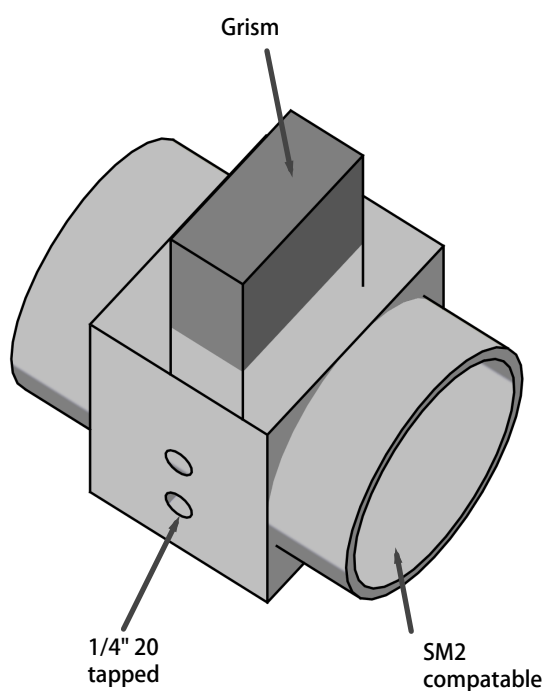
**Collimating optical carriage.**

Delrin box for angling mirrors and objective mounting.

To scale.

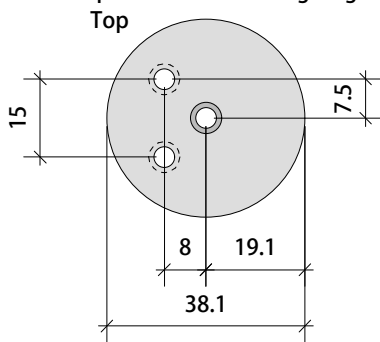


Delrin box for angling mirrors and objective mounting.
To scale.

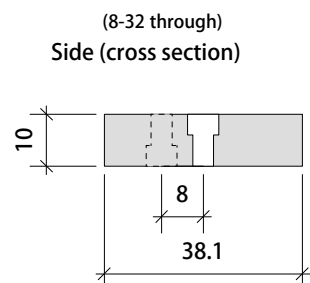


Delrin Mirror Mount for new 2" mirror

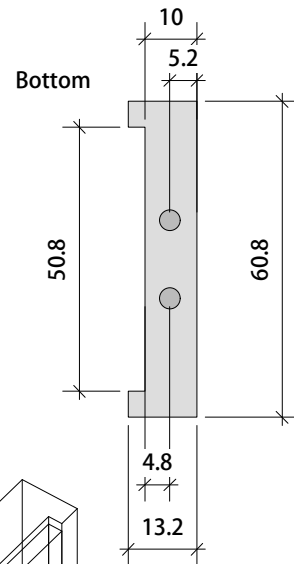
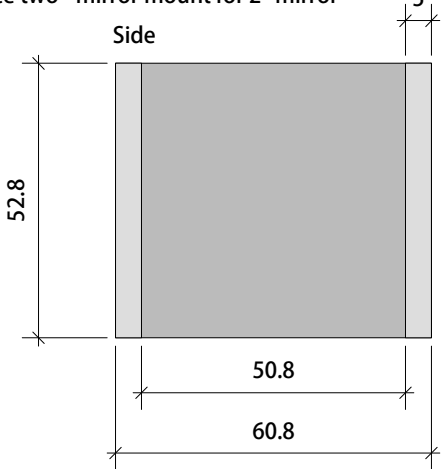
Piece one - adapter for NX1 indexing stage



(8-32 through)
Side (cross section)



Piece two - mirror mount for 2" mirror



Together

